Study of radiation damage in aluminum

E. Verbiest and H. Pattyn
Instituut voor Kern- en Stralingsfysika, K.U.-Leuven, B-3030 Leuven, Belgium
(Received 8 September 1981)

A mathematical model to describe the radiation damage in aluminum is presented. The concentrations of monointerstitials, di-interstitials, interstitial clusters, monovacancies, divacancies, and vacancy clusters, and the average sizes of the clusters are calculated and plotted as a function of the irradiation dose at liquid-helium temperature and the thermal annealing temperature. Any irradiation dose (electron, neutron, heavy ion) is expressed as the number of interstitials or vacancies per atom which has been produced (cipa for created interstitials per atom). Also calculated are the fractions of Co impurities, present in the aluminum, which have trapped one or more interstitials or vacancies. With the use of Mössbauer spectroscopy these fractions are measured experimentally as a function of the dose of a heavy-ion implantation and of the annealing temperature. The unknown parameters in the model, which are mainly trapping volumes, are determined by fitting the calculated values to the experimental data. The model calculations, executed for a large range of irradiation doses and annealing temperatures, reproduce nicely our experimental results as well as results reported by other groups. The calculations indicate that an irradiation dose of 0.001 cipa yields a concentration of interstitials (and vacancies) of almost 0.0007, mainly present as monointerstitials and monovacancies; at 0.01 cipa it is about 0.002, distributed over the various defect configurations; at 0.1 cipa it is about 0.003 with nearly all interstitials in clusters with an average size of about 15 and vacancies still mainly present as monovacancies. The trapping volumes for interstitials are larger than the corresponding ones for vacancies and therefore interstitials cluster more easily than vacancies. Of the Al atoms displaced during the collision cascade produced by one 85-keV Al atom, about 20% is removed outside the volume for recombination with its own vacancy.

I. INTRODUCTION

During irradiation, energetic particles penetrating a solid displace some atoms from their original positions, thus producing vacancy-interstitial pairs (Frenkel pairs). If an atom is not displaced far enough the Frenkel pair is unstable and the interstitial recombines with its own vacancy. With increasing irradiation more and more defects remain in the material and the probability for a vacancy or interstitial to be produced within the trapping volume of a defect already present in the material increases. The trapping volume of a defect A for a defect B is that volume around A in which B always clusters with A. Recombination and trapping volumes are temperature dependent. At high doses nearly all newly produced defects cluster or recombine and the detailed structure of the radiation-induced damage becomes hard to describe. Doses so high are hardly ever reached during electron irradiation, where defects are produced throughout a thick layer of the material and most energy is lost to electronic excitations, but they are readily obtained by heavy-ion implantation where most of the energy is lost by nuclear stopping which produces defects throughout a thin surface layer (typically 1000 Å). The interest in studies of these high doses is not of purely scientific importance but is also vital to technological applications as the development of reactor materials and the various ways in which heavy-ion implantation can be used to change properties of materials or to introduce impurity atoms with a well-controlled dose and depth distribution.

Over the years a number of techniques have been developed to study the radiation damage in metals. Resistometry is most widely used. Measuring the resistivity of a sample allows one to deduce the total number of defects present in the material. This method is very suitable to study in detail the different recovery stages upon annealing, especially the temperature at which they occur and the amount of recovery during each stage. The main drawback of this macroscopic technique is that va-

cancies cannot be distinguished from interstitials. Some techniques are more specific, e.g., through differential dilatometry the total number of vacancies can be measured; channeling is mainly sensitive to interstitials. Through transmission electron microscopy the number and size of large interstitial and vacancy clusters can be determined. Positron annihilation spectroscopy even distinguishes between vacancies, divacancies, and larger clusters. The only technique able to count the interstitials, vacancies, di-interstitials, divacancies, and other small clusters in a sample is field ion microscopy. However, the presence of very large electric fields and the drawback that only surface atomic layers can be peeled off renders this technique less trustworthy to study bulk properties. We conclude that the determination of the detailed structure of radiation damage by looking at the defects themselves poses severe problems.

An alternative approach is to look not at the damage itself but at its interaction with impurities placed as probes in the lattice. Impurities attract and trap some kinds of defects present in their vicinity. The number of defects trapped after a certain irradiation and annealing treatment is related to the total numbers of the different defect structures, their mobilities, and their trapping behavior. We will show how the combination of a mathematical model that describes these relations and experimental measurements yields a detailed description of the radiation damage in aluminum.

As a defect trapping probe we introduce radioactive ^{57}Co into the aluminum, which decays to ^{57}Fe, thereby emitting a 14.4-keV γ ray. The energy of this γ quantum is modified by the electrostatic interactions of the Fe nucleus with its electronic surroundings (hyperfine interactions) which are different for a Fe (Co) atom associated with different kinds of defects. These energy changes of the order of 10^{-8} eV can be measured by Mössbauer spectroscopy (recoilless nuclear resonance absorption). This hyperfine interaction technique gives direct information on the atomic configuration of the first-neighbor shells around the probe atoms and allows us, in principle, to "see" trapped interstitials, vacancies, di-interstitials, divacancies, or other small-defect agglomerates.

II. EXPERIMENTAL MEASUREMENTS

A. Technical details

A polycrystalline aluminum foil with a purity of 99.9999% was prepared from aluminum purchased from the Aluminum Aktien Gesellschaft, Darmstadt. It was mounted in a combicryostat (Leybold Heraeus) allowing it to be cooled to a lowest temperature of 1.6 K by pumping on the liquid helium. Built-in heating elements and thermometers together with a control unit for temperature stabilization allow the temperature of the sample to be stabilized anywhere between 1.6 and 360 K to a precision of about 0.1 K. The vacuum inside the cryostat filled with liquid helium is 2×10^{-7} Torr. The upper part of the cryostat to which the sample holder is attached can be turned around its vertical axis over 360° without influencing this vacuum. To implant heavy ions the vacuum chamber of the cryostat was connected to the target chamber of our isotope separator which has been described by Pattyn.[1] The sample was cooled to liquid-helium temperature immediately before the beginning of each implantation as an extra measure in order to minimize the thickness of a condensation layer. The implantation energy was always 85 keV, while the sample temperature was always 4.2 K. Radioactive ^{57}Co has been implanted first to a dose of 2×10^{14} atoms/cm^2, giving a maximum Co concentration of about 500 ppm. The Co-implanted aluminum sample has been annealed isochronally to 330 K whereafter all Co impurities are on substitutional lattice positions. Then stable Al atoms have been implanted to various doses, some of which were followed by an annealing sequence to 330 K. The dose rate for the radioactive ^{57}Co implantation was about 10^{10} atoms/cm^2 sec and that for Al atoms about 5×10^{11} atom/cm^2 sec. After an implantation the sample was turned over 180° to put it in front of the Mössbauer drive and the γ-ray detector. The cryostat was disconnected from the isotope separator to minimize vibrations. The main parts of the setup are shown in Fig. 1.

^{57}Co decays to ^{57}Fe with a half-life of 270 days allowing the sample to be measured during several months. The 14.4-keV γ rays of the $(3/2)^-\rightarrow(1/2)^-$ transition in ^{57}Fe, used for Mössbauer spectroscopy, were counted by proportional counters. Two $Na_4Fe(CN)_6\cdot10H_2O$ (sodium ferrocyamide or SFC) absorbers with thicknesses of about 0.1 and 0.5 mg ^{57}Fe/cm^2 were used. They were kept at room temperature. The count rate during the measurements was about 500 Hz. The Mössbauer drive (home built) moved the absorber in a triangular mode with an amplitude of 1.5 mm/sec. During each measurement the velocity of the absorber was controlled by measuring simul-

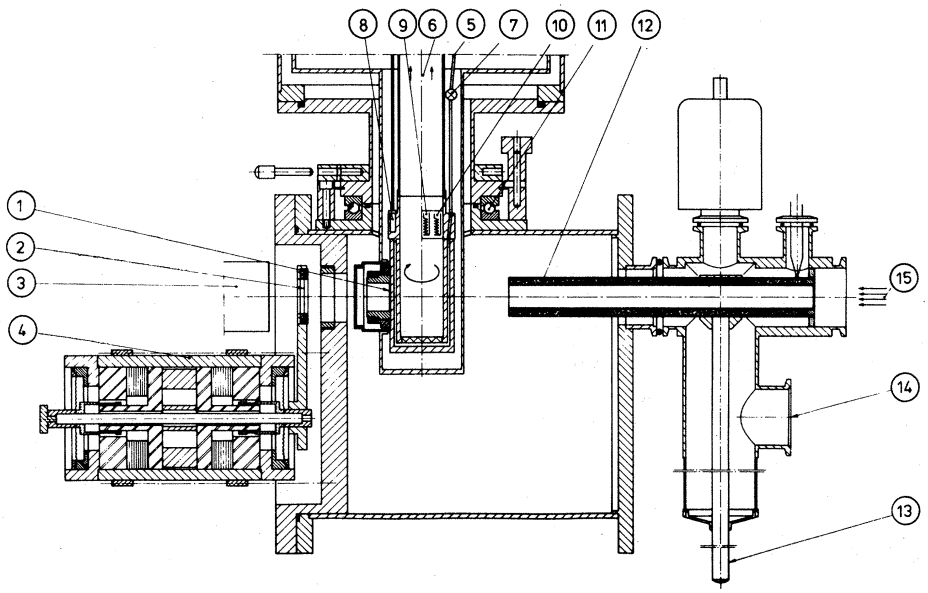

FIG. 1. Main parts of the experimental setup: (1) Mössbauer source, (2) Mössbauer absorber, (3) detector, (4) Mössbauer drive, (5) to the liquid-helium bath, (6) helium-vapor exhaust line, (7) needle valve, (8) vapor-pressure thermometer, (9) thermistor, (10) heater, (11) ball bearing, (12) zeolithe, (13) copper rod to the liquid-nitrogen bath, (14) to the vacuum pump, and (15) ion beam (swept horizontally and vertically).

taneously the Mössbauer spectrum of a ^{57}Co in Cu source mounted on the other end of the drive axis against a thin natural Fe foil as absorber.

Isochronal annealing steps of 30 min have been used. The heating rate was about 0.1 K/sec and the cooling rate about 0.4 K/sec.

All calculations were done on a PDP 11/34 computer. The series of Mössbauer spectra were fitted using the FORTRAN program MOSAUT,[2] which automatically searches a best fit for a series of spectra, and for all other analyses we used the general function and data-analyzing FORTRAN program FDA.[2]

B. Analysis of the Mössbauer spectra

A ^{57}Fe nucleus, produced by the radioactive decay of an implanted ^{57}Co nucleus, has an excited state of 14.4 keV. The width Γ of this energy level is $h/2\pi\tau = 4.7\times10^{-9}$ eV, where τ is the mean lifetime of the excited state. Upon emission of a 14.4-keV γ ray a free ^{57}Fe atom recoils and the γ ray loses an energy of $E_\gamma^2/2m_{\mathrm{Fe}}c^2 = 0.002$ eV. This energy loss is much larger than the width Γ of the energy level and resonant absorption by another ^{57}Fe atom is impossible. If, however, the ^{57}Fe atom is embedded in a lattice, it has a probability f of emitting a γ ray without creating phonons in which case the only energy loss is due to the recoil of the total lattice which is of the order of $E_\gamma^2/2M_{\mathrm{lattice}}c^2 \simeq 10^{-20}$ eV, and thus completely negligible.[3] f is called the recoilless fraction. Recoillessly emitted γ rays are absorbed resonantly by ^{57}Fe atoms in identical lattice positions if this absorption also happens without the creation of phonons. A movement of the source modifies the energy of the γ ray by $E_\gamma v/c = v\times4.8\times10^{-8}$ eV sec/mm, where v is the velocity of the source in mm/sec (Doppler shift). Measurement of the resonant absorption by nuclei embedded in an absorber of γ rays emitted by identical nuclei embedded in a source as a function of the energy difference of the γ transitions (the relative velocity between source and absorber) is called Mössbauer spectroscopy or recoilless nuclear resonance absorption. An absorption line in a Mössbauer spectrum has a Lorentzian shape with a full width at half maximum (FWHM) $W_0 = 2\Gamma$ or $W_0 = 2\Gamma c/E_\gamma$, in velocity units (=0.194 mm/sec) if the source and the absorber are infinitesimally thin. The thickness of our implanted source is negligible. The effective thickness of our absorbers is $t_a = n_a\sigma_0 f_a$, where n_a is the number of ^{57}Fe atoms per cm^2, $\sigma_0 = 2.56\times10^{-18}$ cm^2 is the cross section for resonant absorption,[4] and $f_a = 0.47$ is the recoilless fraction of the absorber at room temperature,[5] giving effective thicknesses of about 1.2 and 6. The line shape

stays approximately Lorentzian and the minimal linewidths become 0.23 and 0.35 mm/sec.[6] Additional line broadening can be caused by unresolved residual hyperfine splittings or experimental effects as uncontrolled source or absorber vibrations, velocity amplitude shifts, and absorber inhomogeneities.

The electrostatic interactions of the ^{57}Fe nucleus with its electronic surroundings, called hyperfine interactions, change the energy of the 14.4-keV level in two ways.[5] First, there is an overall shift of the energy level, called the isomer shift, proportional to $|\Psi(0)|^2$, where $\Psi(0)$ is the electronic density at the nucleus. If the ^{57}Fe nucleus has different electronic surroundings in the Mössbauer source and absorber, the absorption line shifts from the zero velocity position to a position corresponding to an energy proportional to

$$[\,|\Psi_{\text{absorber}}(0)|^2 - |\Psi_{\text{source}}(0)|^2\,] .$$

Second, the 14.4-keV energy level, with spin $\frac{3}{2}$, is split into two levels if an electric field gradient is present at the nucleus. This is the case when the surroundings of the nucleus have a noncubic symmetry. The splitting is proportional to the magnitude of the electric field gradient. Because the 14.4-keV level of the ^{57}Fe in the absorber is not split, ^{57}Fe atoms in the source in positions with electric field gradients give rise to doublets in the Mössbauer spectra.

Fe atoms in the source have different electronic surroundings if their first-neighbor occupation is different. Even after implantations most impurity atoms are only distributed over a few different lattice sites.[7,8] Each site has a well-defined isomer shift, quadrupole splitting, and recoilless fraction. The experimental spectra measured at 4.2 K have been fitted with as few components as possible. Each component had to have the same isomer shift and quadrupole splitting in all spectra. Also the linewidths of all Lorentzians in all spectra measured with the same absorber were forced to be identical. Three components were needed to fit all spectra simultaneously. Their parameters are given in Table I. Typical spectra are shown in Fig. 2. The fitted linewidths were 0.30 and 0.40 mm/sec for the two absorbers used.

The isomer shift is practically temperature independent. Thermal vibrations in the lattice induce a temperature-dependent shift called the second-order Doppler shift.[3] Spectra measured at temperatures above 4.2 K have been fitted with the same second-order Doppler shift for all three components. The quadrupole splitting was also assumed to be temperature independent. Errors due to these approximations are negligible.

The most important result of this fitting procedure is the area under each component in each spectrum. This area is proportional to the number of atoms having the corresponding site configuration multiplied by the recoilless fraction of that site. Because at 4.2 K the recoilless fractions are equal, the relative area under each component is equal to the relative number of Co atoms having the corresponding site configuration. The measured relative site populations are shown in Figs. 6, 7, and 9.

C. Site identification

The component with the most negative isomer shift (−0.64 mm/sec) corresponds to Co atoms placed substitutionally in the lattice. We call this site the *s* site. This component, present in all our spectra, has been described in detail in the literature.[9] The component with an isomer shift of 0.32 mm/sec relative to the substitutional line corresponds to Co atoms associated with one or more vacancies. We call it the *v* site. This component has been observed previously in diffused samples quenched[10–12] to or rolled[13] at liquid-nitrogen or

TABLE I. Parameters of the components in the Mössbauer spectra of a ^{57}Co*Al* source, implanted and measured at 4.2 K, against a $Na_4Fe(CN)_6 \cdot 10H_2O$ absorber at room temperature.

Component	Site	Isomer shift (mm/sec)	Quadrupole splitting (mm/sec)	Site identification
1	*s*	−0.638(4)	0	substitutional Co
2	*v*	−0.32(2)	0.00(2)	Co + vacancies
3	*i*	−0.21(2)	0.16(2)	Co + interstitials

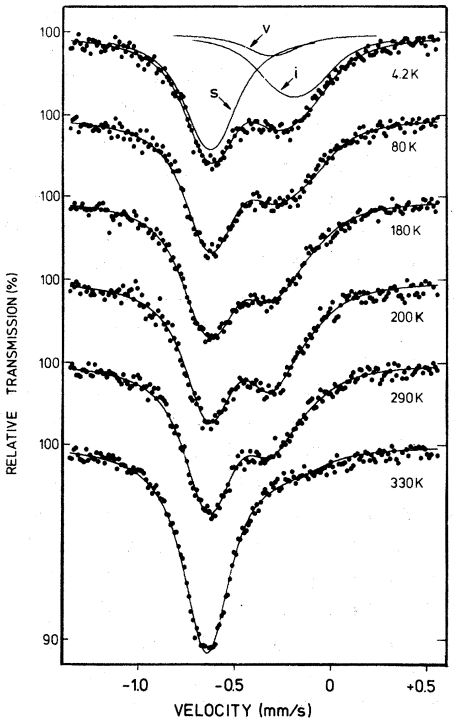

FIG. 2. Mössbauer spectra of a $^{57}CoAl$ source, implanted and measured at 4.2 K, against a $Na_4Fe(CN)_6 \cdot 10H_2O$ absorber at room temperature, after some isochronal (30 min) annealing steps. All spectra are fitted with three components labeled *s*, *v*, and *i* with variable amplitudes.

higher temperatures. The split component with an isomer shift of 0.43 mm/sec relative to the substitutional line corresponds to Co atoms associated with one or more Al interstitials and will be called the *i* site. This component has mainly been observed in diffused samples irradiated with electrons or neutrons at 4.2 K.[14–18] The presence of all three sites *s*, *v*, and *i* in one sample has been reported for the first time after studies of Co implanted in Al at 4.2 K.[19]

After annealing the implanted sample to 500 K a new doublet appears in the Mössbauer spectrum. Other components have also been reported, for instance, in Al-Fe alloys with Fe concentrations[20] above 1 at. % and after implantations of Fe to doses above 10^{15} atoms/cm^2.[21] The formation of all these components, which may correspond to dimers, precipitates, etc., prevent the Co atom to be used to study the radiation damage at higher temperatures.

Although Co atoms associated with one or more interstitials give rise to a component in the Mössbauer spectrum with the same isomer shift and quadrupole splitting it is possible to discern the atoms in an i_1 site (Co associated with one interstitial) from those in an $i_>$ site (Co associated with more interstitials) by recoilless fraction measurements.[17] We have no indication that Co atoms associated with one vacancy can be separated from Co atoms associated with more vacancies by the use of Mössbauer spectroscopy as has been reported.[22]

D. Recoilless fraction measurements

If the atoms in a lattice are assumed to be harmonic oscillators and if the Debye model is used to describe the spectral distribution of the lattice vibration frequencies, the recoilless fraction (*f* fraction) of these atoms can be written as

$$f_{\Theta_D}(T)=\exp\left\{-\frac{6E_R}{k\Theta_D}\times\left[\frac{1}{4}+\left\{\frac{T}{\Theta_D}\right\}^2\int_0^{\Theta_D/T}\frac{x\,dx}{e^x-1}\right]\right\},$$

where T is the temperature, $E_R=E_\gamma^2/2mc^2$ is the recoil energy on emission of a γ ray, k is the Boltzmann constant, and Θ_D is the Debye temperature of the lattice.[3] This Debye model can also be applied if the source atom is an impurity atom by using another Θ_D to account for the frequency changes due to the different mass and force constants.[9] However, an impurity atom can have strong local vibration modes or perform jumps between different lattice sites on a time scale faster than the lifetime of the nuclear state; then the Debye model is no longer applicable.[14,18,23]

We measured the *f* fractions of the three components by recording spectra at various temperatures between 4.2 K and the annealing temperature. The spectra measured at the annealing temperature have been recorded during the last 20 min of the annealing treatment. The *f* fractions of the atoms in the *s* site fit nicely to a Debye model with a Debye temperature $\Theta_D=255(5)$ K, in good agreement with the 250 K reported by Janot for this site.[9] As the isomer shifts of the *v* and *i* components differ only slightly, the areas under both components are strongly correlated and cannot be fitted accurately. The accuracy is improved by taking the area of both components together and by assuming that of these defect sites only the *i* site is present below 160-K annealing and that only the *v* site is present

between 190 and 270 K. The f fractions of the defect sites are shown in Fig. 3. Fitting the f fractions of the v site to the Debye model results in $\Theta_D = 243$ K, but due to the large experimental errors $\Theta_D = 255$ K also gives a reasonable fit. This means that the vibrations of the Co atom are only slightly influenced by the presence of the neighboring vacancies. The total area under all three components at 4.2 K does not depend on the relative amplitudes of the components. So at 4.2 K the f fraction of all sites is identical. At temperatures above 17 K the f fraction of the i site drops suddenly and fits no longer a Debye model with $\Theta_D = 255$ K.

The i site is made up of Co atoms associated with one or more interstitials. Computer calculations[24] predict that a strongly undersized interstitial impurity atom is displaced in the ⟨111⟩ direction a small distance away from the octahedral position. Co is strongly undersized as its effective radius is 1.056 Å against 1.429 Å for the Al atom.[25] Co associated with one interstitial, or more properly said, an interstitial Co atom, called the i_1 site, indeed forms this ⟨111⟩ mixed dumbbell as has been proven by f-fraction measurements along different directions of an Al single crystal.[18] Above 17 K the Co atom starts jumping between the eight equivalent positions of the ⟨111⟩ cube cage, and the f fraction drops suddenly. When the Co atom is associated with more interstitials, called the $i_>$ site, ⟨100⟩ dumbbells are formed.[26] The symmetry is broken and the Co atom can no longer perform jumps between equivalent positions of a cage, and the recoilless fraction increases substantially. Computer calculations indicate that interstitial configurations have strong localized vibration modes,[27,28] and due to this fact the f fraction of the i component stays smaller than that of the s or v component.[29] This peculiar behavior of the f fraction of the interstitial site has also been found for Co in silver.[30]

The difference between the f fractions of the i_1 and $i_>$ site can be used to determine how many atoms reside in each of these sites as has been demonstrated by Mansel.[17] Figure 4 shows his measured f fractions together with the fraction $a_>$ of atoms in the $i_>$ site which he calculated. We used the following model to determine the fraction $a_>$. We assumed that above 20 K the f fractions of the i_1 and the $i_>$ site can both be fitted to a Debye model with Debye temperatures Θ_1 and $\Theta_>$. The total f fraction of the i site is then

$$f_i(T) = a_> f_{\Theta_>}(T) + (1 - a_>) f_{\Theta_1}(T) .$$

We fitted the data of Mansel to this function to find $\Theta_> = 160$ K and $\Theta_1 = 50$ K. The fitted $a_>$ values are listed in Table II and the corresponding

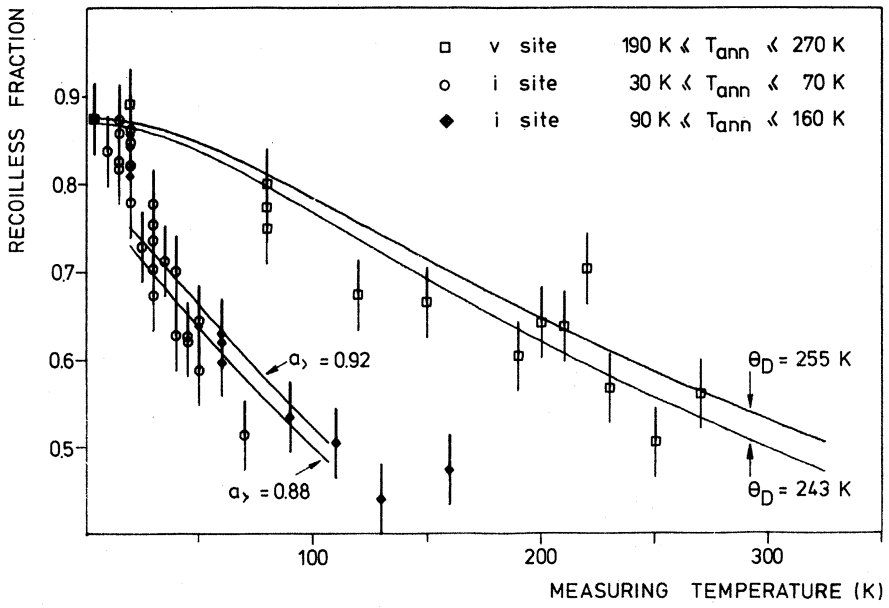

FIG. 3. Recoilless fractions of the defect sites in a $^{57}CoAl$ source, implanted to a dose of 2×10^{14} Co atoms/cm^2 at 4.2 K, after annealing to the indicated temperatures, as a function of the measuring temperature. The f fractions of the v site are fitted to a Debye model.

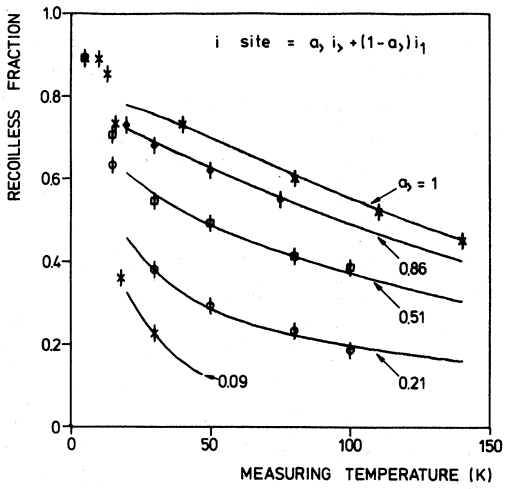

FIG. 4. Recoilless fractions of the i site measured by Mansel (Ref. 17) and the corresponding $a_>$ fractions which he calculated. The data are fitted to $f_i(T) = a_> f_{160}(T) + (1-a_>) f_{50}(T)$ and the fitted $a_>$ values are listed in Table II.

curves are displayed in Fig. 4. The agreement is satisfactory which means that this model can be used. We then obtained the fractions $a_>$ from our measured f fractions for the i site by fitting their values measured above 20 K to $f_i(T)$. The fitted curves are shown in Fig. 4. 88(5)% of the interstitial Co atoms have trapped more than one of the

TABLE II. Fractions of interstitial Co impurities associated with more than one Al interstitials corresponding to f fractions measured by Mansel (Ref. 17) and the fractions obtained after fitting these f fractions to a Debye model assuming Debye temperatures of 50 and 160 K for Co atoms associated with one or more interstitials. The fits are shown in Fig. 4.

$a_>$ data	$a_>$ fitted
0.09(9)	0.08(3)
0.21(9)	0.34(3)
0.51(9)	0.65(3)
0.86(?)	0.86(3)
1.00(?)	0.97(3)

Al interstitials during the Co implantation and this fraction increases only slightly to 92(5)% after annealing above 70 K. These numbers are upper limits because a small part of the f fraction is due to atoms in the v site with a larger f fraction.

In a similar way we analyzed the f fractions of the different components in the sample after an Al postimplantation to a dose of 10^{14} atoms/cm^2. They are shown in Fig. 5. The fitted value for the fraction $a_>$ after stage-I annealing was 90(10)%. The same value was found after an Al postimplantation to a dose of 1.3×10^{15} atoms/cm^2.

Figure 3 also confirms that the i and v sites are

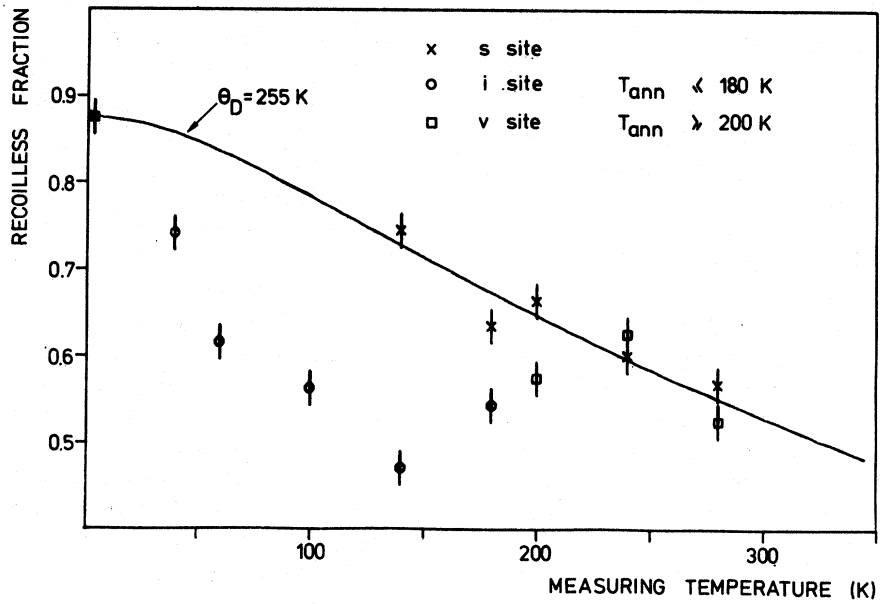

FIG. 5. Recoilless fractions of the substitutional and the defect sites in a source of substitutional Co in Al, postimplanted with 10^{14} Al atoms/cm^2, after annealing to the indicated temperatures, as a function of the measuring temperature. The f fractions of the s site are fitted to a Debye model.

really different sites as their recoilless fractions behave differently in the same temperature region.

E. Thermal annealing behavior

The thermal annealing behavior of Al has been described extensively (see Schilling[31] and references therein). Differential recovery curves obtained by resistivity measurements after neutron irradiation to different doses have been given by Nakagawa.[32] Recovery stage I, at temperatures below 40 K, is due to correlated recovery as well as to the free three-dimensional migration of interstitials.[17,33,34] Annealing stage II, covering the temperature range from 40 to 170 K, is rather complex. The recovery below 100 K, stage II A, is probably due to the migration or dissociation of small interstitial clusters (as di-interstitials), the release of interstitials from shallow traps or the recombination of unstable vacancy-interstitial complexes.[17,31,34–36] The recovery between 100 and 170 K, stage II B, is very small in pure Al but there are several substages if impurities are present in the material.[36,37] Stage II A, with peaks mainly around 45 and 80 K, is probably an intrinsic recovery stage. It increases with increasing defect concentration.[31] Recovery during stage III, from 170 to 260 K, is due to the free migration of vacancies and small vacancy clusters[38] which recombine with interstitials[32] or cluster to form small vacancy clusters at the beginning of this stage and finally form dislocation loops.[39] The presence of impurities acting as nucleation centers increases the loop density.[40,41] No important changes occur in stage IV, between 280 and 350 K. During stage V, from 350 to 450 K, large defect loops become unstable and disappear so that all damage is annealed out.[39]

We study the annealing behavior by measuring as a function of temperature the relative populations of the *s*, *v*, and *i* sites. It is mandatory to know the trapping behavior of the Co impurities for defects to separate the changes of the site populations due to the migration of defects from those due to changes in the trapping behavior. The undersized Co impurity is a strong interstitial trapper[34] and this is not due to elastic interactions only.[42] Some oversized impurities, e.g., In, also trap interstitials.[43] Trapped interstitials are generally released by the impurities around or below stage III,[43–45] but our measurements show that Co impurities keep the interstitials trapped to about 300 K. Most impurities in Al, undersized as well as oversized, also trap vacancies.[46] The Co impurity is once again a strong trapper as it retains the vacancies to about 300 K, whereas the oversized In atom, for instance, releases them around 260 K.[43] It is not surprising that the same impurity traps vacancies as well as interstitials. A vacancy (or interstitial) itself also attracts both kinds of defects. Trapping volumes are temperature dependent, but this has no relevant influence on our results. Also important is the fact that the Co atoms stay immobile at all our annealing temperatures.[47] So defects have to move towards the Co atoms to be trapped and not vice versa. All this shows that the Co impurity is a very suitable probe, as it is sensitive to vacancies as well as interstitials to temperatures above those of stage III, above which all defects are released (which renders the sample usable for another experiment).

Figure 6 shows the site populations during an isochronal annealing sequence (30 min/step) of the sample implanted with Co atoms to a dose of 2×10^{14} atoms/cm^2 These results reproduce those which we obtained earlier from a similar sample.[19] Due to the high dose no free interstitials remain and no stage-I recovery is seen. This also occurs after fast neutron irradiation to doses around 10^{19} neutrons/cm^2.[16] Stage-II recovery occurs between 40 and 80 K. The changes of the *i*- and *v*-site populations, compared to the errors, are rather small to be really convincing. They suggest between 40 and 60 K a conversion of the *v* site to the *i* site, probably caused by the capture of migrating, small interstitial clusters, as expected during stage-II recovery. Between 60 and 80 K, however, the *s* and *v* sites tend to increase at the expense of the *i* site. This means that vacancies or vacancy clusters are trapped or interstitials are pulled away from the Co impurities. So vacancies are involved but no vacancy-type defects are freely mobile at these temperatures. So this recovery may have to do with a rearrangement of vacancy clusters, e.g., the collapse of depleted zones or the elimination of configurations of vacancies and trapped interstitials which become thermally unstable due to their mutual interaction. It is to be noted that a strong recovery of the electrical resistivity around 80 K has not only been found after high dose irradiations[31,32] but also after deformations by compression,[48] torsion,[49], rolling,[50] and extension.[51] The most important changes in the site populations occur between 160 and 240 K with a peak around 180 K. This is recovery stage III. The *i* site is converted to the *s* or *v* sites, and the *s* site is con-

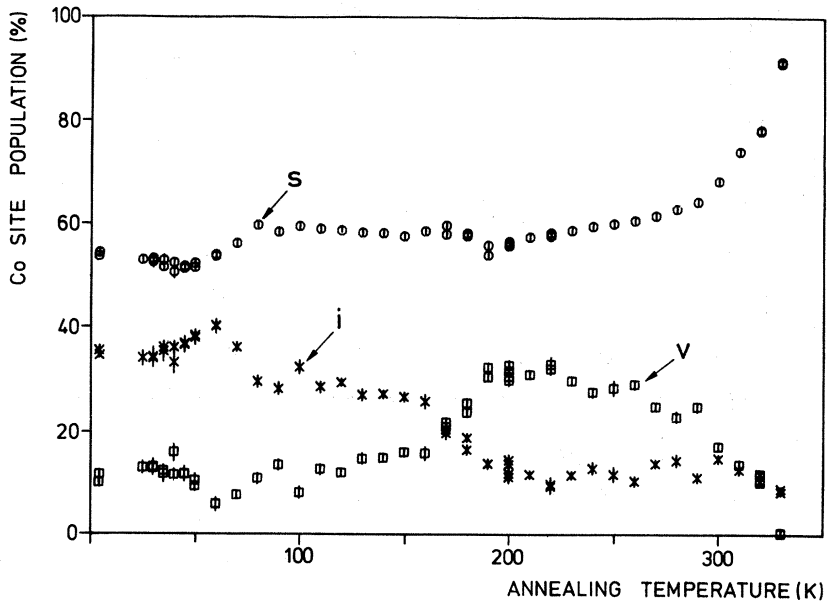

FIG. 6. Relative site populations for Co atoms implanted into aluminum (2×10^{14} atoms/cm^2, 85 keV, 4.2 K) after isochronal annealing steps (30 min).

verted to the v site as freely mobile vacancies and small vacancy clusters are trapped by the Co impurities. The s-site population stays constant due to the dynamical equilibrium between its production and its annihilation. This equilibrium critically depends on the concentrations of the various defects present in the material. Around 290 K, the Co impurities release all defects and nearly all Co atoms end up as substitutional after annealing to 330 K. At this temperature nearly all the irradiation damage is annealed out.[32]

Al atoms have been implanted into this completely annealed sample to doses of (a) 1×10^{14} and (b) 1.3×10^{15} atoms/cm^2. Figure 7 shows some site populations during the isochronal annealing of these samples. Once again no stage-I recovery is observed. Not enough points have been measured to comment on the stage-II recovery. The changes of the site populations during stage-III annealing are clearly dose dependent. After a 1×10^{14}-Al atoms/cm^2 implantation, the s-site population increases by about 20% and the v-site population increases slightly, leading to a large decrease of the i-site population. After a 1.3×10^{15}-Al atoms/cm^2 implantation, the v-site population increases by about 15% at the expense of mainly the s-site population as the i-site population decreases only slightly. As mentioned before the s-site population stays constant at an intermediate dose of 2×10^{14} Co atoms/cm^2 which corresponds to about 5×10^{14} Al atoms/cm^2, as can be seen from Fig. 8 where the damage produced by the implantation of an equal dose of Co and Al atoms at the depth of the implanted Co atoms is plotted against a common (arbitrary) scale.[52]

As this stage-III behavior is strongly dose dependent, it is well suited to test the mathematical model for the radiation damage that we will present further on.

F. Dose dependence

As mentioned above, the changes of the site populations, especially during stage-III annealing, strongly depend on the implantation dose. The site populations immediately after the implantations at 4.2 K also depend on the dose, as shown in Fig. 9. The substitutional site population decreases from 100% to about 50% around a dose of 8×10^{13} Al atoms/cm^2, and then slowly increases to about 60% around 1.3×10^{15} Al atoms/cm^2. The i-site population is maximal where the s-site population is minimal. The v-site population tends to increase slowly. At doses above 10^{14} Al atoms/cm^2, most of the i site consists of Co atoms in the $i_>$ site as shown by the f-fraction measurements.

This behavior will be explained quantitatively by the mathematical model described further on. Qualitatively, the following processes play their part. Interstitials and vacancies are produced. The

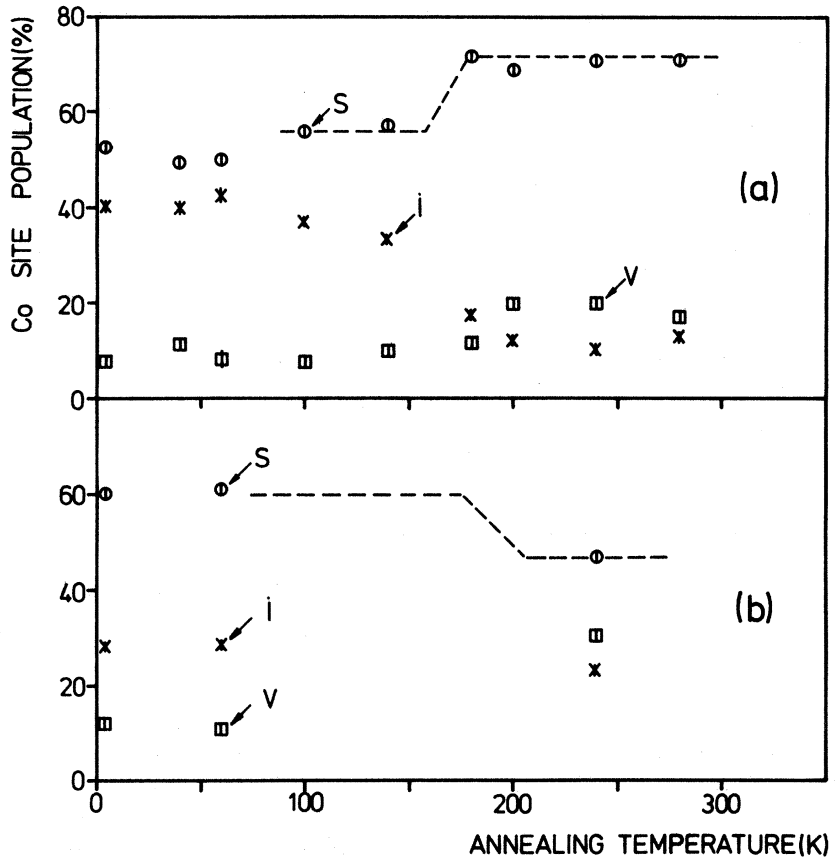

FIG. 7. Relative site populations for Co atoms in Al, initially substitutionally placed, after Al implantations (85 keV, 4.2 K) to doses of (a) 1×10^{14} atoms/cm^2, (b) 1.3×10^{15} atoms/cm^2, and after isochronal annealing steps (30 min).

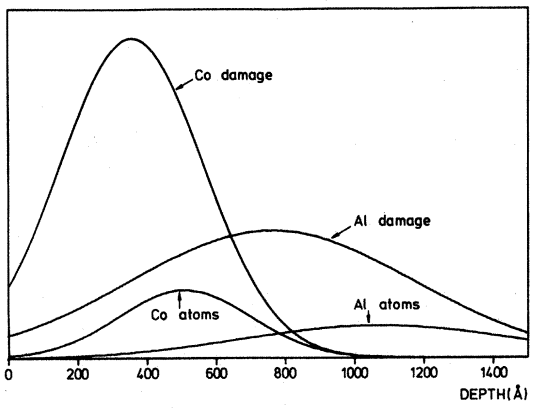

FIG. 8. Gaussian depth distributions of Co ($m=510$, $\sigma=192$) and Al ($m=1074$, $\sigma=392$) atoms implanted into polycrystalline aluminum to the same dose with an energy of 85 keV, and the distributions of the damage they produce (Co: $m=358$, $\sigma=207$; Al: $m=765$, $\sigma=409$) (Ref. 52).

trapping volume of a Co atom for interstitials is much larger than that for vacancies. So at lower doses mainly interstitials are trapped. But because interstitials cluster more easily than vacancies, they are mainly found, upon further dose increase, in clusters, while vacancies still survive as monovacancies. With its trapping volume for recombination being lower when an interstitial sits in a larger cluster than in a smaller one, a further dose increase will concentrate the interstitials in larger and larger clusters, at the expense of the smaller ones, finally decreasing the number of interstitial clusters. The Co impurities which, at the beginning of the irradiation, captured a small number of interstitials take part in the same process, which means that the smaller Co interstitial clusters see their interstitial content readily annihilated by the newly created vacancies, while only the larger ones have a fair chance of survival. When the last in-

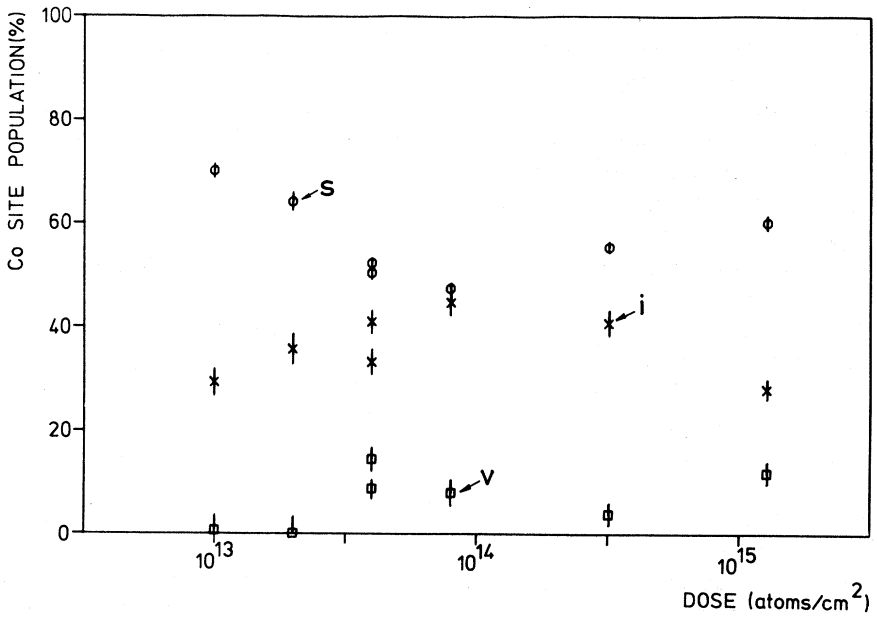

FIG. 9. Relative site populations for Co atoms in Al, initially substitutionally placed, after Al implantations (85 keV, 4.2 K) to various doses.

terstitial of a small cluster around a Co atom is annihilated by a vacancy, the trapping volume of this Co site for vacancies decreases substantially. Because Co atoms in the v site are very effective interstitial trappers, the v-site population increases too slowly to make up for the decrease of the i-site population and so the substitutional Co population increases at higher doses.

III. A MATHEMATICAL MODEL FOR THE RADIATION DAMAGE IN ALUMINUM

A. The outlines

We want to calculate what the radiation damage in Al looks like as a function of the irradiation dose, if the irradiation is performed at a low temperature where all defects are immobile. We characterize the damage by the concentrations of interstitials, vacancies, di-interstitials, divacancies, and interstitial and vacancy clusters and their average sizes. We assume that during an irradiation process vacancies and interstitials are produced in equal numbers and at random places in the material. The irradiation dose is expressed as the concentration of created interstitials (or vacancies), not taking into account the spontaneous recombination. When an interstitial (or vacancy) is created inside the trapping volume of an already existing defect, it combines with this defect. With increasing dosage, more and more defects are present in the material and the probability for a newly created point defect of being inside the trapping volume of another defect increases. The following reactions are possible during the irradiation process: $I+I$, I_2+I, I_C+I, $V+I$, V_2+I, V_C+I, $V+V$, V_2+V, V_C+V, I_2+V, and I_C+V, where the abbreviations I, I_2, I_C, V, V_2, and V_C stand for interstitial, di-interstitial, interstitial cluster, vacancy, divacancy, and vacancy cluster, respectively. The probability that, for instance, V, when created, reacts as I_2+V is proportional to the product of the trapping volume of a di-interstitial for a vacancy and the concentration of di-interstitials in the material. Thus, the radiation damage as a function of the dose is described by a set of rate equations with the trapping volumes of all defects as parameters. These parameters have to be adjusted by fitting the calculated values to experimental results.

Our experimental results are Co-site populations. So we calculate the Co-site populations using the calculated defect concentrations. We treat the Co atom just as an atom probing the volume of the material. We set the fraction of Co atoms which have trapped two interstitials equal to the probability that a Co atom at a random place in the lattice is situated inside the trapping volume of a di-

interstitial for a Co atom; or put another way, set it equal to the fraction of the volume occupied by the trapping volume of all di-interstitials for Co atoms. We believe that this approximation is justified because the Co atoms remain immobile in the lattice and have to undergo all the defect creation and annihilation reactions, and because our maximum Co concentration of about 500 ppm is small enough not to have an important influence on the calculated defect concentrations. In reality, however, the Co atoms will compete with the other defects present to trap the newly produced point defects, thus lowering our calculated substitutional site populations. The Co impurities introduce some additional trapping volumes as parameters to be fitted.

Once the structure of the damage at a certain dose is calculated, a thermal annealing simulation can be started. We assume that only I, I_2, V, and V_2 are mobile and allow each of these defects to react with each of the six monitored defect types. Changing the concentration of a defect C due to a reaction $A+B\rightarrow C$ is assumed to be proportional to the product of the concentrations of A and B and the sum of the jump frequencies of A and B. All influences due to reactions with impurities, rearrangements, or breakdowns of defect structures and thermally produced defects are neglected. In this way only the main features of stage-I and stage-III recovery are simulated. To reproduce the experimentally measured Co-site populations, the four migrating defect species are allowed to interact with the existing Co sites. In principle, the migration enthalpies of the defects appear as additional parameters in the model, but because they are known well enough and because we are not really interested in the thermal positions of the recovery stages and only in the changes they inflict on the site populations, they are not to be fitted.

The model outlined here is of course a substantial simplification of real nature, where, for instance, trapping volumes are temperature dependent and overlap at higher doses, where the produced damage and the Co impurities are not distributed homogeneously, where there are small equilibrium vacancy concentrations, where defects react with impurities, where the lattice structure influences cluster forms, etc. We believe, however, that the mechanisms that dominate the damage production and annealing through stage I and III are included. Apart from a description of the radiation damage and different trapping volumes other information will be gained, such as the number of Frenkel pairs produced by one implantation cascade. The following section describes the model in detail and the next one lists the results. Different uses of rate equations in connection with radiation damage have already been proposed in the literature.[53–59]

B. Detailed description

1. *Damage production during the irradiation*

The temperature is low enough for no defects to be freely mobile. An irradiation creates damage in a volume of N atomic volumes. A single irradiating particle creates inside this volume, P Frenkel pairs, not taking into account the spontaneously recombining interstitials and vacancies. These P interstitials and P vacancies are supposed to be produced in an uncorrelated way at random places inside the volume of N atoms. $P\Phi$ is the total number of Frenkel pairs produced inside the volume of N atoms, when the fluence of irradiating particles is Φ. Irradiation doses will be expressed as $P\Phi/N$ which represents the total number of created defects per atomic volume (cipa for created interstitials per atom). Φ is a continuously changing variable in the calculation. With regard to heavy-ion implantation, the calculation is only useful when the fluence is high enough for the total volume to be filled with damage cascades (a dose of 10^{11} to 10^{12} atoms/cm^2).

Calculated are the concentrations of interstitial defects: n_I/N, the number of I per N atoms; n_{I_2}/N, the number of I in I_2 per N atoms; n_{I_C}/N, the number of I in I_C per N atoms; N_{nI_C}/N, the number of I_C per N atoms; and the corresponding concentrations for vacancies: n_V/N, n_{V_2}/N, n_{V_C}/N, and n_{nV_C}/N. The average size of clusters of three or more interstitials is $\lambda_I=n_{I_C}/n_{nI_C}$ and for vacancies $\lambda_V=n_{V_C}/n_{nV_C}$.

Parameters are the following trapping volumes, which are all expressed in aluminum atomic volumes: v_R, the recombination volume for an I and a V; v_{II}, I for I; v_{I_2I}, I_2 for I per I of I_2 ($=\frac{1}{2}$ of the total trapping volume of the I_2); v_{I_CI}, I_C for I per I of the cluster; v_{V_2I}, V_2 for I per V of V_2; v_{V_CI}, V_C for I per V of the cluster; and the corresponding trapping volumes for vacancies: v_{VV}, v_{V_2V}, v_{V_CV}, v_{I_2V}, and v_{I_CV}. Of those only v_R, v_{II}, v_{VV}, v_{V_2I}, and v_{I_2V} are independent parameters to

be fitted. We assume, as a simple model to account for overlapping trapping volumes, that the trapping volume of a defect in a cluster decreases as the square root of the cluster size. This choice will be discussed in Sec. III C 1. So the trapping volume of a cluster of j interstitials for an interstitial is $j(v_{I_jI})=j(v_{II}/j^{1/2})=j^{1/2}v_{II}$. This leads to $v_{I_2I}=v_{II}(\frac{1}{2})^{1/2}$, $v_{I_CI}=v_{II}(1/\lambda_I)^{1/2}$, $v_{V_CI}=v_{V_2I}(2/\lambda_V)^{1/2}$, $v_{V_2V}=v_{VV}(\frac{1}{2})^{1/2}$, $v_{V_CV}=v_{VV}(1/\lambda_V)^{1/2}$, and $v_{I_CV}=v_{I_2V}(2/\lambda_I)^{1/2}$. Two additional parameters α and β are included to allow the creation of larger vacancy clusters during one implantation cascade (depleted zones). α is the fraction of the vacancies produced as single vacancies in one cascade and β is the average size of the formed vacancy clusters and has to be equal or larger than three.

The probability for a newly produced I (or V) to react with an existing defect X is equal to the fraction of the volume covered by the trapping volume of X for the I and can be written as n_Xv_{XI}/N, where n_X/N is the concentration of defects X and v_{XI} is the trapping volume of X for I. The possible overlap of trapping volumes v_{XI} is neglected. Eleven different clustering reactions make the following probability terms appear in the rate equations: $V+I$, $ai=n_Vv_R/N$; $I+V$, $av=n_Iv_R/N$; $I+I\rightarrow I_2$, $bi=n_Iv_{II}/N$; $V+V\rightarrow V_2$, $bv=n_Vv_{VV}/N$; $V_2+I\rightarrow V$, $ci=n_{V_2}v_{V_2I}/N$; $I_2+V\rightarrow I$, $cv=n_{I_2}v_{I_2V}/N$; $I_2+I\rightarrow I_C$, $di=n_{I_2}v_{I_2I}/N$; $V_2+V\rightarrow V_C$, $dv=n_{V_2}v_{V_2V}/N$; $V_C+I\rightarrow V_C$ or V_2, $ei=n_{V_C}v_{V_CI}/N$; $I_C+V\rightarrow I_C$ or I_2, $ev=n_{I_C}v_{I_CV}/N$; $I_C+I\rightarrow I_C$, $fi=n_{I_C}v_{I_CI}/N$; and $V_C+V\rightarrow V_C$, $fv=n_{V_C}v_{V_CV}/N$. The result of the cluster annihilation reactions V_C+I and I_C+V is distributed over the di-defect and defect clusters by assuming that the probability of formation of the di-defect is inversely proportional to the cluster size.

The rate equations describing the damage production are listed in Table III. These equations are numerically integrated. All defect concentrations are put equal to zero for zero irradiation dose.

TABLE III. Set of rate equations describing the damage production at low temperatures where no defects are mobile. All abbreviations are explained in Sec. III B 1.

$dn_I/Pd\Phi=$	1	$-ai$	$-\alpha av$	$-2bi$		$-ci$	$+\alpha cv$	$-di$		$-ei$			$-fi$	
$dn_V/Pd\Phi=$	α	$-ai$	$-\alpha av$		$-2\alpha bv$	$+ci$	$-\alpha cv$		$-\alpha dv$		$-\alpha ev$			$-\alpha fv$
$dn_{I_2}/Pd\Phi=$				$+2bi$			$-2\alpha cv$	$-2di$			$+2\alpha ev/\lambda_I$			
$dn_{V_2}/Pd\Phi=$					$+2\alpha bv$	$-2ci$			$-2\alpha dv$	$+2ei/\lambda_V$				
$dn_{I_C}/Pd\Phi=$								$+3di$			$-\alpha ev-2\alpha ev/\lambda_I$		$+fi$	
$dn_{V_C}/Pd\Phi=$	$(1-\alpha)$								$+3\alpha dv$	$-ei-2ei/\lambda_V$				$+\alpha fv$
$dn_{n_{I_C}}/Pd\Phi=$								$+di$			$-\alpha ev/\lambda_I$			
$dn_{n_{V_C}}/Pd\Phi=$	$(1-\alpha)/\beta$								$+\alpha dv$	$-ei/\lambda_V$				

2. *Co-site populations during the irradiation*

Calculated are the fractions of the Co atoms which are associated with an I (n_{CI}), an I_2 (n_{CI_2}), an I_C (n_{CI_c}), a V (n_{CV}), a V_2 (n_{CV_2}), and a

V_C (n_{CV_C}). The fraction of substitutional Co atoms (n_C) contains all other Co atoms. Defects are produced and annihilated throughout the lattice. The Co atom does not migrate to seek out the defects but has to wait until defects are produced inside its trapping volume. If v_{C_I} represents the trapping volume of an interstitial for a Co atom (or vice versa) then a fraction $n_I v_{CI}/N$ of the total volume is covered by the trapping volume of Co impurities for I. The probability of a randomly placed Co atom of being associated with an I is equal to this volume fraction. In this way the Co impurities (whose concentration is small) just act as observers without any influence on the damage. In reality the Co atoms compete actively with the other defects already present for the possession of the newly produced defects. Neglecting this phenomenon will probably render our substitutional Co-site population a little bit too high.

Once again trapping volumes appear as parameters. v_{CI} is the trapping volume of an I for a Co impurity, $2^{1/2}v_{CI}$ that of an I_2, $\lambda_I^{1/2}v_{CI}$ that of an I_C, and correspondingly for vacancies we have v_{CV}, $2^{1/2}v_{CV}$ and $\lambda_V^{1/2}v_{CV}$.

The site populations are not described by rate equations but are directly proportional to the defect concentrations:

$$n_{CI}=n_I v_{CI}/N ,$$

$$n_{CI_2}=n_{I_2}v_{CI}/2^{1/2}N ,$$

$$n_{CI_C}=n_{I_C}v_{CI}/\lambda_I^{1/2}N ,$$

$$n_{CV}=n_V v_{CV}/N ,$$

$$n_{CV_2}=n_{V_2}v_{CV}/2^{1/2}N ,$$

$$n_{CV_C}=n_{V_C}v_{CV}/\lambda_V^{1/2}N ,$$

$$n_C=1-(n_{CI}+n_{CI_2}+n_{CI_C}+n_{CV}+n_{CV_2}+n_{CV_C}) .$$

These site populations, like the defect concentrations, can be fitted to experimental results to obtain the values of the parameters.

3. *Damage evolution during a thermal annealing simulation*

The damage was produced by irradiation at a temperature where all defects are immobile (i.e., 5 K). When the temperature is raised some defects start wandering through the lattice until they penetrate the trapping volume of another defect and then they combine. The evolution of the defect concentrations clearly depends on the initial defect concentrations. Four defects are allowed to migrate: I, I_2, V, and V_2. We express their jump frequencies as

$$\nu_I=\nu_0\exp(-E_I^m/kT) ,$$

$$\nu_{I_2}=\nu_0\exp(-E_{I_2}^m/kT) ,$$

$$\nu_V=\nu_0\exp(-E_V^m/kT) ,$$

and

$$\nu_{V_2}=\nu_0\exp(-E_{V_2}^m/kT) ,$$

where k is the Boltzmann constant, T the temperature, ν_0 the attempt frequency, and E_I^m, $E_{I_2}^m$, E_V^m, and $E_{V_2}^m$ are the migration enthalpies of the various defects. In principle the five additional parameters, ν_0, and the migration enthalpies can be fitted to the experimental data. They determine at what temperatures the main concentration changes occur. However, their values are known well enough and in this work we are interested not in the temperatures at which the concentration changes occur but in the magnitude of the changes. So we treat them as constants with values: $\nu_0=10^{14}$, $E_I^m=0.115$ eV, $E_{I_2}^m=0.135$ eV, $E_V^m=0.60$ eV, and $E_{V_2}^m=0.45$ eV.

The probability of occurrence for the reaction $X+Y\rightarrow Z$, which we denote as X^*Y, is proportional to the product of the concentrations of X and Y, $n_X n_Y/N^2$. It is also proportional to the relative migration velocities of X and Y. Whichever of both is mobile is not important. Setting $X^*Y \sim(\nu_X+\nu_Y)n_X n_Y/N^2$ simplifies the notations without doing any harm. The proportionality factor depends on factors as the magnitude of the trapping volume v_{XY}, on the amount of correlated jumps and on the heating rate. As we do not want to fit ν_0 and the migration enthalpies, κv_{XY} will do, with κ fitted to the experimental results to put the recovery stages in the right temperature ranges. So the concentration changes due to the reaction $X+Y$ are

$$\frac{dn_X}{Ndt}=-X^*Y=-\kappa v_{XY}(\nu_X+\nu_Y)n_X n_Y/N^2 ,$$

$$\frac{dn_Y}{Ndt}=-X^*Y ,$$

$$\frac{dn_Z}{Ndt}=+X^*Y .$$

An isothermal annealing sequence is simulated by the integration of the rate equations with constant jump frequencies corresponding to the annealing temperature. The experimental isochronal annealing sequence is not simulated by a discrete number of isothermal annealing steps but instead by a constant heating rate $\theta=dT/dt$. Then, at any moment, the temperature T is proportional to the time t elapsed since the start of the annealing treatment and the jump frequencies at any moment are written as

$$\nu_X=\nu_0\exp(-E_X^m/k\theta t) .$$

The set of rate equations describing the evolution of the damage during the thermal annealing simulation is listed in Table IV.

Some additional approximations are made. The number of clusters is kept constant during annealing, unless the average cluster sizes λ_I or λ_V drop below three. In that case the number is put equal to $n_{I_C}/3$ or $n_{V_C}/3$. The average cluster size is needed to evaluate some trapping volumes. As yet undefined trapping volumes for I_2 are approximated as $v_{I_2I_2}=v_{I_2I}$, $v_{I_CI_2}=v_{I_CI}$, $v_{V_2I_2}=v_R$, $v_{V_CI_2}=v_{V_CI}$, and correspondingly for V_2.

4. *Co-site populations during a thermal annealing simulation*

The Co-site populations change during the thermal annealing because the mobile defects are trapped when they meet a Co atom. The Co atoms stay immobile at all temperatures. So the probability of occurrence for a reaction $X+CY\rightarrow CZ$ can be written as

$$X^*CY=\kappa v_{CYX}\nu_X n_X n_{CY}/N^2 .$$

The trapping volume of the Co site CY for the mobile defect X, v_{CYX}, is v_{CI} or v_{CV} when CY represents substitutional Co and is otherwise assumed to be equal to the trapping volume of the defect that is formed if the Co atom is substituted with an Al atom (i.e., $v_{CII}=v_{II}$, $v_{CVI}=v_R$,...). The Co-site concentrations are proportional to the total Co-impurity concentrations. We performed the calculations assuming a very low Co concentration of 20 ppm. This Co concentration or the corresponding trapping volumes are of little importance as they mainly influence the thermal positions of the recovery stages which are not to be fitted to experimental results. The concentration changes of the seven different Co sites are

TABLE. IV. Set of rate equations describing the defect concentrations during a thermal annealing treatment. The abbreviations are explained in Secs. III B 1 and III B 3.

$dn_I/Ndt=$	$+V^*I_2$	$-I^*I$	$-I_2^*I$	$-I_C^*I$	$-V^*I$	$-V_2^*I$	$-V_C^*I$				
$dn_{I_2}/Ndt=$	$-2V^*I_2$	$+I^*I$	$-2I_2^*I$					$-I_2^*I_2$	$-I_C^*I_2$	$-V_2^*I_2$	$-V_C^*I_2$
$dn_{I_C}/Ndt=$			$+3I_2^*I$	$+I_C^*I$			$-V^*I_C$	$+I_2^*I_2$	$+I_C^*I_2$		$-I_C^*V_2$
$dn_V/Ndt=$	$-V^*I_2$	$-V^*V$	$-V_2^*V$	$-V_C^*V$	$-V^*I$	$+V_2^*I$	$-V^*I_C$				
$dn_{V_2}/Ndt=$		$+V^*V$	$-2V_2^*V$			$-2V_2^*I$		$-V_2^*V_2$	$-V_C^*V_2$	$-V_2^*I_2$	$-I_C^*V_2$
$dn_{V_C}/Ndt=$			$+3V_2^*V$	$+V_C^*V$			$-V_C^*I$	$+V_2^*V_2$	$+V_C^*V_2$		$-V_C^*I_2$

described by the set of rate equations listed in Table V.

Separating the damage annealing from the Co-site annealing, as we did, is only allowed when the Co concentrations are much smaller than the defect concentrations. We believe that the Co concentration of maximum 500 ppm in our experimental samples is small enough to justify this as a rough approximation.

5. Fitting procedure

All sets of equations have been integrated numerically. Good results have been obtained by assuming that no depleted zones are formed in a one-collision cascade, this means $\alpha=1$ and β of no importance. The results are rather insensitive to α and β as long as $\alpha \geq 0.5$. Mainly four calculated curves have been used to determine the seven other parameters of the model, namely the substitutional Co-site populations as a function of the dose and as a function of the annealing temperature after three irradiation doses. The corresponding experimentally measured curves (Figs. 6, 7, and 9) are the most accurate ones. Emphasis has been put not on the absolute magnitudes but on the magnitudes of the changes. The calculations have been done using a large number of parameter sets. The results obtained with the parameter sets giving the best agreement with the experimental results, are presented in the next section.

C. Calculated results

1. Trapping volumes

Table VI shows the trapping volumes giving the best agreement between the calculated and the experimental results. The results are more sensitive to the ratios of v_{II}, v_{VV}, v_{V_2I}, v_{I_2V}, v_{CI}, and v_{CV} than to their absolute values, and rather insensitive to the value of v_R. $v_{R=300}$ also produces a good fit. The error on the ratios of the trapping volumes is estimated to be about 10% and the error on the magnitudes to be about 20%.

The assumption that the trapping volume of a defect in a cluster decreases as (cluster size)$^\eta$ with $\eta=\frac{1}{2}$ is rather arbitrary. We also performed some calculations with $\eta=\frac{1}{3}$ and $\frac{2}{3}$. The results with $\eta=\frac{1}{2}$ and $\frac{2}{3}$ do not differ much and seem slightly better for $\eta=\frac{1}{2}$. However, really fitting this value

TABLE V. Set of rate equations describing the Co-site populations during a thermal annealing treatment. The abbreviations are explained in Secs. III B 1–III B 4.

$dn_C/Ndt=$	$+V{*}CI+I{*}CV+V_2{*}CI_2+I_2{*}CV_2-I{*}C-V{*}C-I_2{*}C-V_2{*}C$
$dn_{CI}/Ndt=$	$-V{*}CI+I{*}C+V{*}CI_2+I_2{*}CV-V_2{*}CI+V_2{*}CI_C-I{*}CI-I_2{*}CI$
$dn_{CI_2}/Ndt=$	$-V_2{*}CI_2+I_2{*}C-V{*}CI_2+V_2{*}CI_C+I{*}CI+V{*}CI_C-I{*}CI_2-I_2{*}CI_2$
$dn_{CI_C}/Ndt=$	$-2V_2{*}CI_C+I_2{*}CI-V{*}CI_C+I{*}CI_2+I_2{*}CI_2$
$dn_{CV}/Ndt=$	$-I{*}CV+V{*}C+I{*}CV_2-I_2{*}CV+V_2{*}CI+I_2{*}CV_C-V{*}CV-V_2{*}CV$
$dn_{CV_2}/Ndt=$	$-I_2{*}CV_2+V_2{*}C-I{*}CV_2+I_2{*}CV_C+V{*}CV+I{*}CV_C-V{*}CV_2-V_2{*}CV_2$
$dn_{CV_C}/Ndt=$	$-2I_2{*}CV_C+V_2{*}CV-I{*}CV_C+V{*}CV_2+V_2{*}CV_2$

TABLE VI. Trapping volumes determined by fitting calculated Co-site populations to experimentally measured ones, expressed in Al atomic volumes or related to other trapping volumes.

$v_R(=v_{IV})$	400	
v_{II}	200	$v_R/2$
v_{VV}	133	$v_R/3$
v_{V_2I}	210	$3/2\ v_{I_2I}$
v_{I_2V}	140	$3/2\ v_{V_2V}$
v_{CI}	250	
v_{CV}	50	$v_{CI}/5$

makes sense only when more realistic models are used as the influence of this parameter is comparable to that of some approximations used. The unsaturable trap model ($\eta=1$) cannot account for the dose dependence of the Co-site populations.

2. *Damage production during the irradiation*

Figure 10 shows the radiation damage calculated with the trapping volumes of Table VI. Interstitials have a strong tendency to cluster. Only at low doses (0.005 cipa) do I or I_2 dominate. Of 100 created interstitials per 1000 atoms (0.1 cipa), three interstitials remain and they are all present as clusters of three or more interstitials with an average cluster size of about 15. At doses above 0.02 cipa the number of interstitial clusters decreases and the cluster size starts to increase more rapidly. Most of the vacancies, however, survive as single vacancies even at doses above 0.1 cipa and the average size of the vacancy clusters does not increase. Figure 11 shows the damage calculated with $v_R=300$. The defect concentrations reached are about 15% higher than the corresponding concentrations for $v_R=400$.

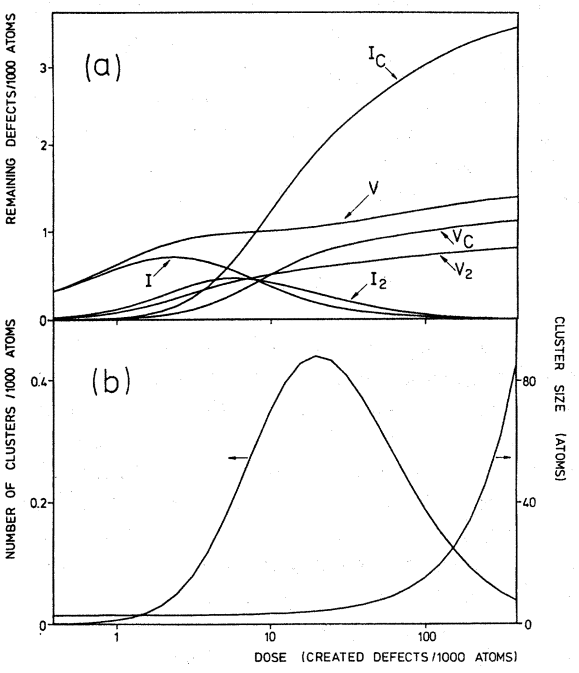

FIG. 10. Calculated damage (using the parameters of Table VI) as a function of the irradiation dose, characterized by the numbers of interstitials and vacancies present as point defects or as clusters of two or more defects (a) and by the number of clusters of three or more interstitials and their average size (b).

3. *Co-site populations during the irradiation*

Figure 12 shows the Co-site populations which have to be compared to the experimental values shown in Fig. 9. This comparison allows a dose calibration; 0.02 cipa corresponds to 1×10^{14} 85-keV Al atoms/cm^2. The i_1-site populations which forms part of the i-site population is shown also. As determined experimentally by f-fraction measurements the calculations indicate that at doses above 0.02 cipa most of the i site is made up by Co atoms associated with more than one Al interstitial. If in the model the Co atoms would be allowed to compete with the defects for the possession of the newly produced defects, the slope of the s-site population would always be somewhat more negative which would improve the agreement with the experimental results.

Figure 13 shows the populations calculated with $v_R=300$ and $v_{CI}=200$. The results are nearly identical and the same dose calibration can be used. At doses around 10^{14} atoms/cm^2, cascades

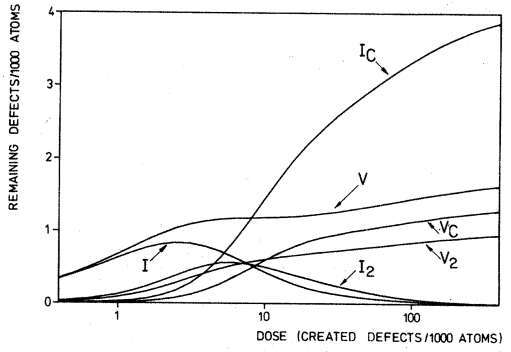

FIG. 11. Calculated defect concentrations (using $v_R=300$) as a function of the irradiation dose.

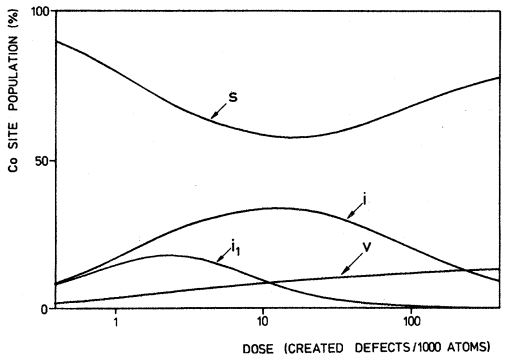

FIG. 12. Calculated relative site populations for Co atoms in Al, initially substitutionally placed, as a function of the irradiation dose (using the parameters of Table VI).

heavily overlap and the results are determined by the trapping volumes governing the clustering processes.

4. *Damage evolution during a thermal annealing simulation*

Figure 14 shows the number of defects as a function of the irradiation dose and the annealing temperature. The curves on the extreme right are those of Fig. 10 (defects against irradiation dose). At various dose points an isochronal annealing sequence up to 300 K is simulated.

The changes of the interstitial defect concentrations [Figs. 14(a)—14(c)] first increase to doses of about 0.005 cipa. Then they decrease and at doses above 0.1 cipa no stage-I recovery remains to be seen. The changes of the vacancy defect concentrations [Figs. 14(d)—14(f)] become larger and larger with increasing dose. The recovery stages shift to lower temperatures with increasing dose.

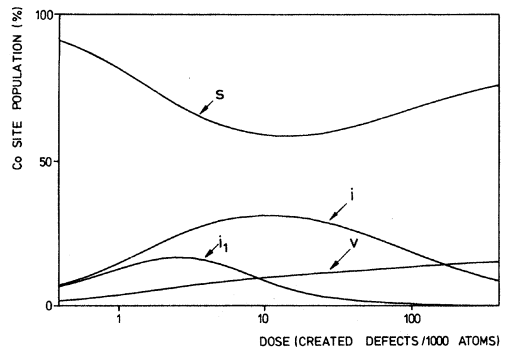

FIG. 13. Calculated relative Co-site populations as a function of the irradiation dose (using $v_R = 300$ and $v_{CI} = 200$).

5. *Co-site populations during a thermal annealing simulation*

Figure 15 shows the substitutional Co-site population as a function of the irradiation dose and the annealing temperature. The curves corresponding to doses of 1×10^{14}, 5×10^{14}, and 13×10^{14} Al atoms/cm^2 are to be compared to the experimental results of the Figs. 6 and 7. Using the formerly derived calibration, 0.02 cipa $=1\times10^{14}$ Al atoms/cm^2, these doses are 0.02, 0.1, and 0.26 cipa (they are marked by arrows in the figure). The strong suppression of stage-I annealing and the unorthodox behavior of the *s*-site population during stage-III annealing are in good agreement with the experimental results which are unable to separate the changes due to mono- and divacancy migration.

Figure 16 shows the corresponding defect associated Co-site populations i_1, i, v_1, and v. As experimentally measured hardly any changes in the i-site population occur after high-dosage irradiations and at our experimental doses nearly all Co atoms in the i site are associated with more than one Al interstitials. It is also apparent that the v_1 site remains rather small at all doses and all annealing temperatures. The increase of the v-site population during stage-III annealing is nearly completely due to the increase of the $v_>$-site population.

IV. DISCUSSION

The correspondence between our calculated and experimental results is quite satisfactory. This is not sufficient proof for the rightness of the model because a large part of the correspondence results from a fitting procedure. To evaluate the model we compare the obtained results to some data from the literature. If our calculations reproduce experimentally measured facts that have in no way been used to adapt parameters of our model, we may hope that also the predictions which have not yet been verified experimentally, are sound.

A. Trapping volumes

Many values have been reported for the recombination volume v_R. In most cases they have been

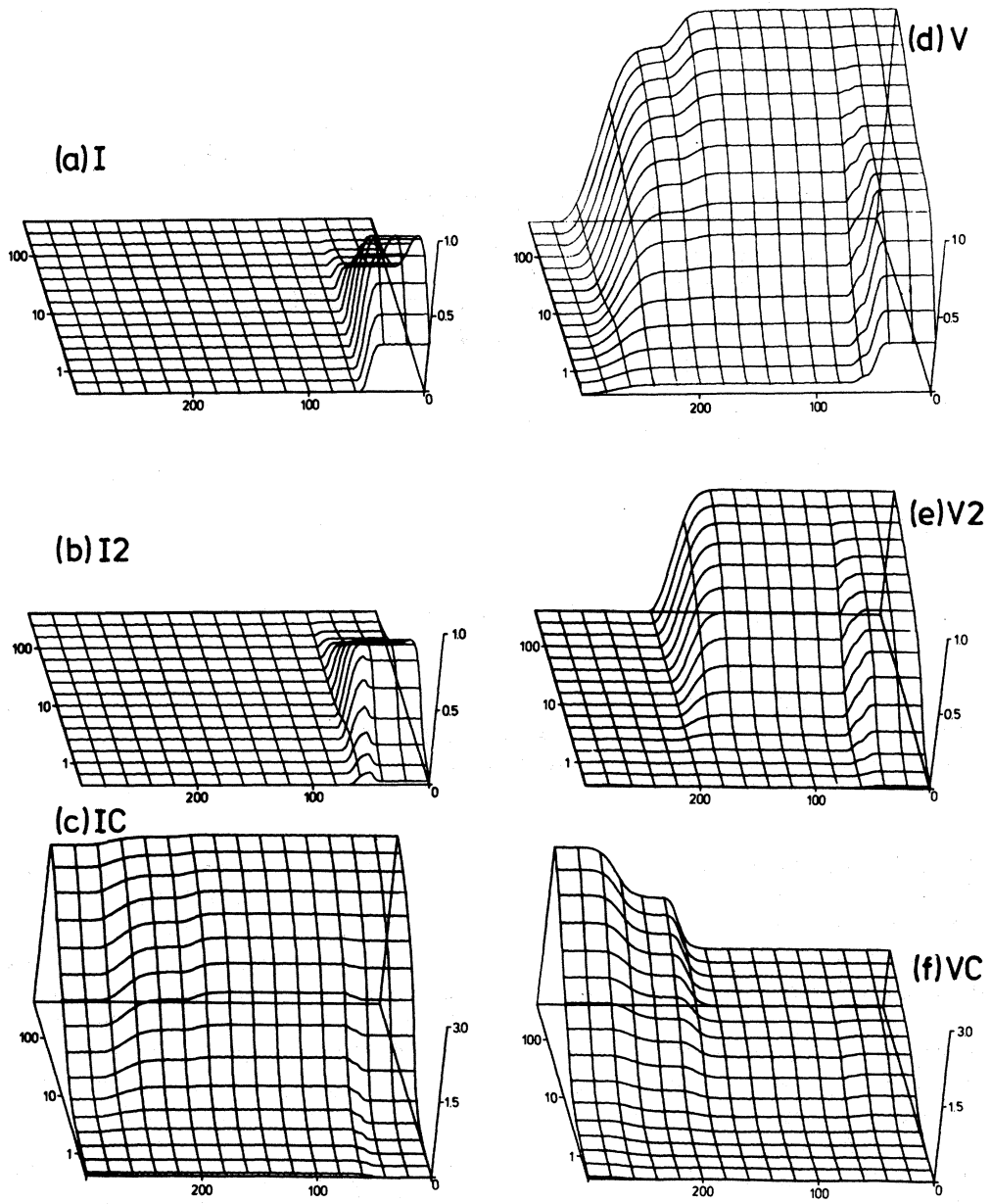

FIG. 14. Calculated defect concentrations as a function of the irradiation dose and the annealing temperature (using the parameters of Table VI). Concentrations are expressed in remaining defects/1000 atoms, the dose in created defects/1000 atoms, and the annealing temperatures in K.

derived by measuring resistivity changes as a function of the irradiation dose. The resistivity increase per unit concentration of Frenkel defects is about $4.4\times10^{-4}\ \Omega\,\mathrm{cm}$.[56] So the defect concentration as a function of the dose is measured and this is fitted to models containing the recombination volume v_R. Obtained values range from 100 to 150 after electron irradiation,[60] 170 to 240 after heavy-ion irradiations,[61] and after neutron irradiations, 115 (Ref. 62) or 150 to 450.[32] The large spread in v_R is not due to uncertainties in the data but results mainly from the differences in the models used to analyze the data. Computer calculations put 74 atoms inside the recombination

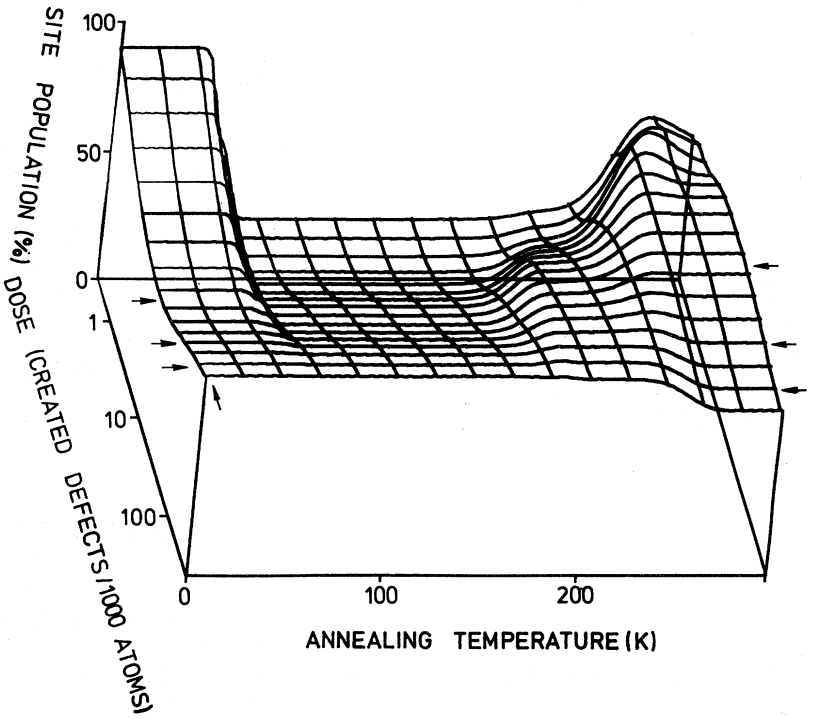

FIG. 15. Calculated population of Co atoms substitutionally placed in Al after irradiations to different doses followed by isochronal annealing sequences (using the parameters of Table VI). Arrows indicate the curves corresponding to the experimentally measured values shown in Figs. 6, 7, and 9.

volume.[27] Larger values have also been reported, i.e., a sphere of 3.5 lattice units radius containing about 680 atoms.[59] The values of 300 and 400 which we propose are on the high side of the v_R values. Our results are rather insensitive to the value of v_R.

Values of other defect-defect trapping volumes are harder to obtain. v_{II} has been reported to be a sphere of 9 lattice units radius.[59] Compared to our results this value is much too large. Attempts have been made to obtain values such as $v_{I_2 I}$ but experimental errors are too large to allow a definite determination.[63]

More is known about the trapping volumes of impurities for interstitial Al atoms. Channeling measurements using Ag in Al indicate that at 70 K, v_R is 4 to 5 times larger than this trapping volume,[45,64] but more frequently ratios between 1 and 2 are reported.[42,65–67] A value of $v_{CI}=200$ has been derived by Mansel[16] by comparing the change of the i-site population measured by Mössbauer spectroscopy to the change of the electrical resistivity after neutron irradiations. By fitting the same data after calculating the number of produced Frenkel pairs to a rate equation model $v_{CI}=195$ has been obtained.[68] So the value of 200 to 250 and the ratio of $v_R/v_{CI}=1.5$ to 2 which we propose seem to be realistic. Less information is available on the trapping volume for vacancies. In any case v_{CV} is much smaller than v_{CI} because immediately after an irradiation the v-site population is always much smaller than the i-site population.

The trapping volumes in our model are those during the irradiation at 4.2 K and take into account dynamical effects. A possible explanation for the fact that the trapping volume for an interstitial is always larger than the corresponding one for a vacancy is that the interstitial is displaced by, for instance, a focused collision sequence. Thus, it scans a part of the lattice, has a better chance of meeting a reaction partner, and acquires a larger trapping volume.

B. Calibration of irradiation doses

Results of irradiations by electrons, neutrons, and heavy ions can only be compared if their doses are expressed on a common scale. A suitable scale is the total number of Frenkel pairs produced in a volume divided by the total number of atoms in

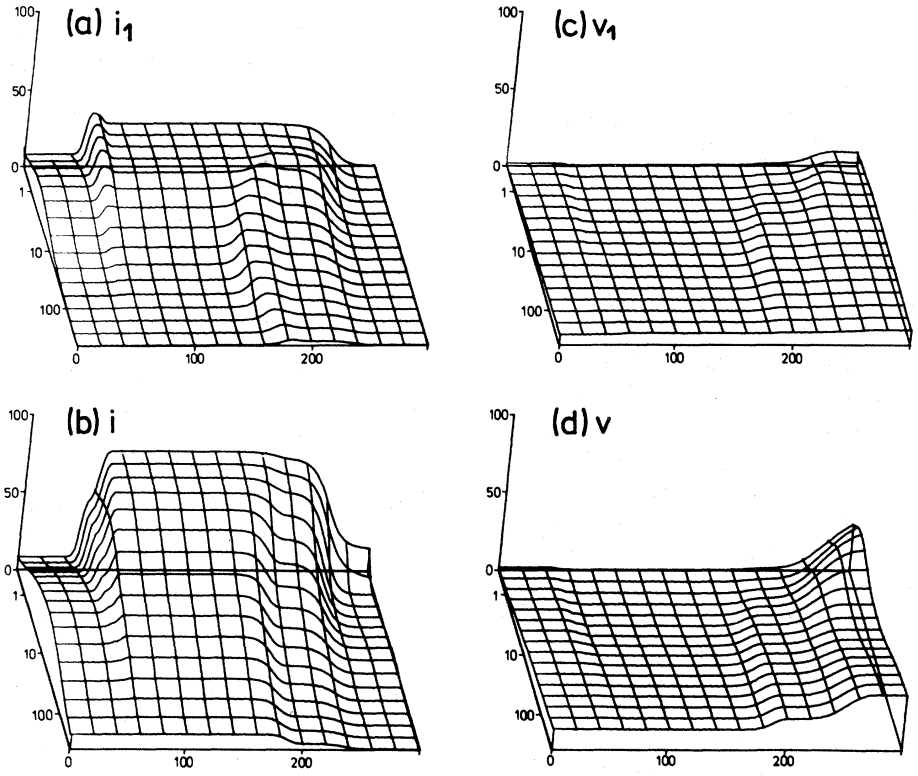

FIG. 16. Calculated populations of Co atoms in the i_1, i, v_1, and v sites as a function of the irradiation dose and the annealing temperature (using the parameters of Table VI). The populations are expressed as percentages, the doses in created defects/1000 atoms and the annealing temperatures in K.

that volume, abbreviated cipa (defects per atom). As mentioned in Sec. III C 3, a dose of 1×10^{14} 85-keV Al atoms/cm^2 corresponds to 0.02 cipa. According to Wurm the resistivity increment per unit dose for a 3-MeV electron is about 1.08×10^{-26} Ω cm^3 and 0.6×10^{-26} Ω cm^3 for a 1-MeV electron.[69] So 10^{18} 3-MeV electrons/cm^2 correspond to $10^{18}\times1.08\times10^{-26}/4.4\times10^{-4}=25\times10^{-6}$ cipa. 10^{18} 1-MeV electrons/cm^2 is about 15×10^{-6} cipa. However, Mansel[17] associates 10^{18} 2.8-MeV electrons/cm^2 to 5×10^{-6} cipa. 0.7×10^{18} fast neutrons ($E\geq0.1$ MeV)/cm^2 induce a resistivity change of 1.8×10^{-7} Ω cm.[17] So 10^{18} fast neutrons/cm^2 correspond to 58×10^{-6} cipa.

The number ν of Frenkel pairs produced by one incoming 85-keV Al atom in aluminum is now easily determined. As Fig. 8 shows, 85-keV Al atoms produce their damage in a layer of about 1500-Å thickness containing 9×10^{17} atoms/cm^2. Calculating ν,

$$\frac{\nu\times10^{14}\ \text{cascades/cm}^2}{9\times10^{17}\ \text{atomic volumes/cm}^2}=0.02\frac{\text{defects}}{\text{atomic volume}}\rightarrow\nu=180\ .$$

About 40 keV of the energy is lost by nuclear stopping (E_n) and produces Frenkel pairs.[52] 16 eV (E_d) is needed to displace an Al atom.[70,71] According to the modified Kinchin-Pease rule,[72] $0.8E_n/2E_d=1000$ atoms are displaced in one cascade of a 85-keV Al atom in aluminum. Only 180 of those remain. Thus, about 20% of the displaced atoms are removed outside the volumes for recombination with their own vacancies and can remain as interstitials in the lattice. By resistivity measurements effective displacement energies of 45 to 60 eV have been found after electron irradiations, and around 60 eV after neutron or deuteron irradiations.[56,69] With $E_d=16$ eV, this means that about 30% of displaced atoms do not recombine with their own

vacancies. So 20% for heavy ions is a reasonable number. One neutron would produce 0.0035 remaining Frenkel pairs per micron in aluminum.

C. Comparison of our calculated results to other experiments

Mansel measured Co-defect-site populations (i site+v site) for different neutron irradiation doses between 0.2×10^{18} and 7.3×10^{18} neutrons/cm^2 as a function of the annealing temperature.[16] His measured populations 3%, 10%, 20%, and 55% for doses of 0.0001, 0.0004, 0.0013, and 0.0042 cipa, respectively, agree well with our calculated 3%, 10%, 23%, and 36%. Two differences are found in the annealing behavior: First, stage-I recovery is suppressed at doses somewhat lower; and second, the changes during stage-I annealing are somewhat smaller for a dose of 0.0001 cipa than for 0.0004 cipa. These differences are not so important, but might indicate that our ratio of v_{II}/v_{CI} is somewhat too small.

Mansel also measured the i_1- and $i_>$-site populations as a function of the annealing temperature after a neutron irradiation of 0.7×10^{18} neutrons/cm^2.[17] They are reproduced by the calculations.

Kalish implanted 4×10^{14} 100-keV Al atoms/cm^2 in aluminum with a low Co concentration and studied the annealing behavior using backscattering and channeling.[47] His results agree with our experimental and calculated results.

Using perturbed angular correlation the structure of the impurity-vacancy (In instead of Co) site in Al has been investigated.[73,74] The structure mainly shows a ⟨111⟩ symmetry, pointing to impurities associated with two or more vacancies. This can be explained. The substitutional impurity has a small trapping efficiency for vacancies, so it is difficult to form the v_1 site. As soon as a vacancy is trapped, the trapping efficiency increases drastically due to the vacancy. This enables the conversion of most of the v_1 site to the $v_>$ site [see Figs. 16(c) and 16(d)].

The vacancy concentration in Al after irradiations at 4.6 K with fast (1×10^{18} neutrons/cm^2) and thermal neutrons (1.6×10^{18} neutrons/cm^2), and after annealing to 125 K, has been measured by the muon spin-rotation technique as 30×10^{-5} and by resistivity measurements as 25×10^{-5}.[75] Our calculations give 15×10^{-5} at 0.001 cipa and 25×10^{-5} at 0.0015 cipa, which deviates by at most a factor of 2 from the experimental results.

Transmission electron microscopy shows that during electron irradiation interstitial loops grow, whereas vacancy loops are annihilated by trapping interstitials.[40] The calculations predict large interstitial clusters at high doses and no large vacancy clusters.

A good fit to our measurements was possible without taking into account a certain amount of vacancy clustering in the cascade ($\alpha=1$). This agrees with experiment.[76,77]

D. Possible further developments

Although many approximations have been made, the calculated results reproduce the experimental results remarkably well. The method outlined here serves as a base suitable for further refinements. The sets of rate equations describing the damage production and the annealing are easily combined by expressing the dose as a function of time and adding both sets. A more detailed description of the damage production at a certain irradiation temperature is obtained by taking the thermal equilibrium defect concentrations into account.[54,78] The overlap of trapping volumes during the irradiation can be taken into account. A newly produced I can land inside the trapping volume of, i.e., both an I_C and a V_2. The inclusion of this phenomenon, which becomes more important with increasing dose, would increase the concentrations of V and I. It can be done by writing the trapping volumes as a function of the volume fractions occupied by the trapping volumes of the various defects. Less important during the irradiation are the reactions between defects which occur when a cluster grows until its trapping volume reaches other defects. The temperature dependence of the trapping volumes can be included by substituting a trapping volume v_Q by, for example, $v_Q T^\tau$ in a certain temperature range.[79] Fitting to experimental results then allows to test models for this temperature dependence. The trapping volumes during the irradiation and the annealing can be made different to include dynamical effects by, i.e., using $(v_{Q_{\text{dynamic}}}+v_{Q_{\text{static}}})$ in the damage production equations and $v_{Q_{\text{static}}}$ in the annealing equations. More refined models for the dependence on the cluster size of the trapping volume per clustered defect than the square root of the size that we used can be elaborated. When heavy-ion implantations are investigated the depth dependence of the produced damage or the implanted impurities may be included. The model can be extended to describe in detail the

formation of clusters of three, four, or more defects. Impurity-defect-site populations during irradiation and annealing can both be written as sets of rate equations and both can be combined with the sets of equations for the damage production. This is necessary to investigate the dependence of the damage structure on the impurity concentrations.

This list of refinements is not exhaustive. Most refinements are easily included as they only require the addition of certain terms to the equations or the substitution of variables by functions in the computer programs. All rate equations are numerically integrated and as fast digital computers are nowadays readily available the complexity of the equations is of little importance. It is however most important to have enough accurate experimental results to check the calculated results or to determine unknown parameters by a fitting procedure. Model calculations will point out which experiments are most sensitive to certain effects, thus increasing the experimental efficiency.

An advantage of this method over the more classical technique of resistivity measurements to determine trapping volumes is that nothing has to be known about the resistivity increase per unit concentration of Frenkel defects. Results obtained by this method can be used to check various assumptions about these resistivity increases.

V. CONCLUSIONS

We have proposed a simplified mathematical model to describe the evolutions of the defect concentrations in Al during an irradiation and a subsequent thermal annealing treatment. This model also describes the population changes of various impurity-defect agglomerates. Experimentally we have measured in an accurate way such population changes using Mössbauer spectroscopy and we have used these results to determine the unknown parameters in the model and to check it. We have also compared our calculated values to other experimental results. The very good agreement between theory and experiment is partly due to the fact that the fit was run with many fit parameters and that a number of other parameters was suitably fixed. We feel, however, that this number of parameters is not too large considering that many curves have to be reproduced simultaneously. In this way results obtained by quasimicroscopic methods sensitive to the atomistic environment of probe atoms can be used to study macroscopic properties such as the various defect concentrations.

The calculations indicate that during an irradiation interstitials cluster more easily than vacancies. At high doses (about 0.1 cipa) nearly all interstitials are present in clusters which decrease in number but grow in size, whereas most of the vacancies still survive as single vacancies. Large vacancy clusters are not formed. Various trapping volumes have been determined and those for interstitials are larger than the corresponding trapping volumes for vacancies.

To compare results obtained after irradiations with electrons, neutrons and heavy ions we expressed their doses as the number of defects (interstitials or vacancies) produced per atom (cipa). 10^{18} 3-MeV electrons/cm^2 $=25\times10^{-6}$ cipa, 10^{18} fast neutrons/cm^2 $=580\times10^{-6}$ cipa, and 10^{12} 85-keV Al atoms/cm^2 $=200\times10^{-6}$ cipa. Of the Al atoms displaced during the collision cascade of one 85-keV Al atom, about 20% are moved outside the recombination volume of its own vacancy and can remain as interstitials in the lattice.

In view of the success of this simple model, more detailed models should be constructed and their skeleton computer programs distributed so that various models to describe various influences can be easily inserted. The models can then be tested as comparable experimental results become available and vice versa calculations can predict which experimental results are most sensitive to which parameters.

ACKNOWLEDGMENTS

The authors gratefully acknowledge the cooperation of Dr. J. Odeurs in the construction of the experimental equipment. The Al foils were prepared by Dr. A. Stesmans. This work has been supported financially by the Interuniversitair Instituut voor Kernwetenschappen.

[1]H. Pattyn, Ph.D thesis, Katholieke Universiteit Leuven (unpublished).

[2]E. Verbiest, unpublished.

[3]V. G. Bhide, *The Mössbauer Effect and its Applications* (Tata McGraw-Hill, New Dehli, 1973).

[4]*Mössbauer Effect Data Index,* edited by J. G. Stevens and V. E. Stevens (Plenum, New York, 1976), p. 51.

[5]T. C. Gibb, *Principles of Mössbauer Spectroscopy*

(Chapman and Hall, London, 1976).
[6]J. Heberle, Nucl. Instrum. Methods 58, 90 (1968).
[7]S. R. Reintsema, E. Verbiest, J. Odeurs, and H. Pattyn, J. Phys. F 9, 1511 (1979).
[8]E. Verbiest, H. Pattyn, and J. Odeurs, Nucl. Instrum. Methods 182-183, 515 (1981).
[9]C. Janot and H. Gibert, Philos. Mag. 27, 545 (1973).
[10]H. Ichinose, K. Sassa, Y. Ishida, and M. Kato, Philos. Mag. 36, 1367 (1977).
[11]K. Sassa, H. Goto, Y. Ishida, and M. Kato. Scr. Metall. 11, 1029 (1977).
[12]H. Ichinose, K. Sassa, Y. Ishida, and M. Kato, Scr. Metall. 11, 539 (1977).
[13]R. S. Preston, S. Nasu, and U. Gonser, J. Phys. (Paris) 40, C2-564 (1979).
[14]G. Vogl, W. Mansel, and W. Vogl. J. Phys. F 4, 2321 (1974).
[15]W. Mansel, G. Vogl, and W. Koch, Phys. Rev. Lett. 31, 359 (1973).
[16]W. Mansel and G. Vogl, J. Phys. F 7, 253 (1977).
[17]W. Mansel, H. Meyer, and G. Vogl, Radiat. Eff. 35, 69 (1978).
[18]W. Petry, G. Vogl, and W. Mansel, Phys. Rev. Lett. 45, 1862 (1980).
[19]E. Verbiest, H. Pattyn, and J. Odeurs, J. Phys. (Paris) 41, C1-431 (1980).
[20]S. Nasu, U. Gonser, P. H. Shingu, and Y. Murakami, J. Phys. F 4, L24 (1974).
[21]B. D. Sawicka, M. Drwiega, J. Sawicki, and J. Stanek, Hyperfine Int. 5, 147 (1978).
[22]S. Umeyama, K. Sassa, M. Taniwaki, Y. Ishida, and H. Yoshida, in *Proceedings of the Fifth International Conference on Hyperfine Interactions, Berlin, 1980,* edited by G. Kaindl and H. Haas (North-Holland, Amsterdam, 1981), p. 705.
[23]H. J. Lipkin, Ann. Phys. (New York) 26, 115 (1964).
[24]P. H. Dederichs, C. Lehmann, H. R. Schober, A. Scholz, and R. Zeller, J. Nucl. Mater. 69-70, 176 (1978).
[25]C. Dimitrov and O. Dimitrov, C. R. Acad. Sci. Ser. C 266, 304 (1968).
[26]H. R. Schober, J. Phys. F 7, 1127 (1977).
[27]A. Scholz and C. Lehmann, Phys. Rev. B 6, 813 (1972).
[28]P. H. Dederichs, C. Lehmann, and A. Scholz, Phys. Rev. Lett. 31, 1130 (1973).
[29]G. Vogl, J. Phys. (Paris) 35, C6-165 (1974).
[30]G. Vogl, W. Mansel, W. Petry, and V. Gröger, Hyperfine Int. 4, 681 (1978).
[31]W. Schilling, G. Burger, K. Isebeck, and H. Wenzl, in *Vacancies and Interstitials in Metals,* edited by A. Seeger, D. Schumacher, W. Schilling, and J. Diehl (North-Holland, Amsterdam, 1970), p. 255.
[32]M. Nakagawa, K. Böning, P. Rosner, and G. Vogl, Phys. Rev. B 16, 5285 (1977).
[33]H. M. Simpson and R. L. Chaplin, Phys. Rev. 178, 1166 (1969).
[34]C. Dimitrov, in *Proceedings of the International Conference on Fundamental Aspects of Radiation Damage in Metals, Gatlinburg, Tennessee, 1975,* edited by M. T. Robinson and R. W. Young (National Technical Information Service, Springfield, Virginia, 1975), p. 608.
[35]K. H. Robroc, L. E. Rehn, V. Spiric, and W. Schilling, Phys. Rev. B 15, 680 (1977).
[36]C. Dimitrov, F. Moreau, and O. Dimitrov, J. Phys. F 5, 385 (1975).
[37]C. Dimitrov, O. Dimitrov, H. Mayer, and K. Böning, Phys. Status Solidi A 13, K141 (1972).
[38]R. W. Balluffi, J. Nucl. Mater. 69-70, 240 (1978).
[39]W. R. Wampler and W. B. Gauster, J. Phys. F 8, L1 (1978).
[40]B. L. Eyre, J. Phys. F 3, 422 (1973).
[41]Y. Shimomura and S. Kuwabara, J. Phys. Soc. Jpn. 42, 1221 (1977).
[42]F. Dworschak, C. Dimitrov, and O. Dimitrov, J. Phys. F 8, L153 (1978).
[43]H. Rinneberg, W. Semmler, and G. Antesberger, Phys. Lett. 66A, 57 (1978).
[44]C. Dimitrov, O. Dimitrov, and F. Dworschak, J. Phys. F 8, 1031 (1978).
[45]M. L. Swanson, L. M. Howe, and A. F. Quenneville, Nucl. Instrum. Methods 170, 427 (1980).
[46]R. Yamamoto, O. Tokai, and M. Doyama, J. Phys. F 3, L61 (1973).
[47]R. Kalish and L. C. Feldman, in *Ion Implantations in Semiconductors,* edited by F. Chernow, J. A. Borders, and D. K. Brice (Plenum, New York, 1976).
[48]C. Panseri, R. Ceresara, and T. Federighi, Nuovo Cimento 14, 1223 (1963).
[49]S. Ceresara, H. Elkholy, and T. Federighi, Philos. Mag. 12, 1105 (1964).
[50]C. Frois, Acta Metall. 14, 1325 (1966).
[51]M. L. Swanson, Can. J. Phys. 42, 1890 (1964).
[52]D. K. Brice, *Ion Implantation Range and Energy Deposition Distributions* (Plenum, New York, 1975), Vol. 1.
[53]J. S. Koehler, in *Vacancies and Interstitials in Metals,* Ref. 31, p. 169.
[54]J. Leteurtre, in *Site Characterization and Aggregation of Implanted Atoms in Materials,* edited by A. Perez and R. Coussement (Plenum, New York, 1980), p. 265.
[55]G. Lück and R. Sizmann, Phys Status Solidi 5, 683 (1964).
[56]H. J. Wollenberger, in *Vacancies and Interstitials in Metals,* Ref. 31, p. 215.
[57]K. P. Chik, in *Vacancies and Interstitials in Metals,* Ref. 31, p. 183.
[58]J. Odeurs, R. Coussement, and H. Pattyn, Hyperfine Int. 3, 461 (1977).
[59]H. M. Simpson and A. Sosin, Radiat. Eff. 3, 1 (1970).
[60]G. Duesing, W. Sassin, W. Schilling, and H. Hemmerich, Cryst. Lattice Defects 1, 55 (1969); 1, 135 (1970).
[61]R. S. Averback, K. L. Merkle, and L. J. Thompson, Radiat. Eff. 51, 91 (1980).

[62]O. Dimitrov, C. Dimitrov, P. Rosner, and K. Böning, in *Proceedings of the International Conference on Fundamental Aspects of Radiation Damage in Metals, Gatlinburg, Tennessee, 1975,* Ref. 34, p. 80.
[63]F. Dworschak, B. Schlenger, and H. Wollenberger, Radiat. Eff. 35, 83 (1978).
[64]M. L. Swanson and L. M. Howe, Radiat. Eff. 41, 129 (1979).
[65]F. Dworschak, Th. Monsau, and H. Wollenberger, J. Phys. F 6, 2207 (1976).
[66]R. Rizk, P. Vajda, F. Maury, A. Lucasson, and P. Lucasson, J. Appl. Phys. 47, 4740 (1976).
[67]F. Dworschak, R. Lennartz, Th. Monsau, and H. Wollenberger, in *Proceedings of the International Conference on Fundamental Aspects of Radiation Damage in Metals, Gatlinburg, Tennessee, 1975,* Ref. 34, p. 601.
[68]J. Odeus, dissertation, Katholieke Universiteit Leuven (unpublished).
[69]J. Wurm, F. Dworschak, H. Schuster, and H. Wollenberger, Radiat. Eff. 5, 117 (1970).
[70]P. Vajda, Rev. Mod. Phys. 49, 481 (1977).
[71]P. Lucasson, in *Proceedings of the International Conference on Fundamental Aspects of Radiation Damage in Metals, Gatlinburg, Tennessee, 1975,* Ref. 34, p. 42.
[72]M. T. Robinson, Consultant Symposium Physics of Irradiated Voids, Harwell, 18 (1974).
[73]H. Rinneberg and H. Haas, Hyperfine Int. 4, 678 (1978).
[74]H. G. Müller, in *Proceedings of the International Conference on Point Defects and Defect Interactions in Metals, Kyoto, 1981* (in press).
[75]K. Dorenburg, M. Gladisch, D. Herlach, W. Mansel, H. Metz, H. Orth, G. zu Putlitz, A. Seeger, W. Wahl, and M. Wigand, Z. Phys. B 31, 165 (1978).
[76]M. Wilkens, in *Vacancies and Interstitials in Metals,* edited by A. Seeger, D. Schumacher, W. Schilling, and J. Diehl (North-Holland, Amsterdam, 1970), p. 485.
[77]C. B. Beevers and R. S. Nelson, Philos. Mag. 8, 1189 (1963).
[78]R. W. Siegel, J. Nucl. Mater. 69-70, 117 (1978).
[79]H. Wollenberger, in *Proceedings of the International Conference on Fundamental Aspects of Radiation Damage in Metals, Gatlinburg, Tennessee, 1975,* Ref. 34, p. 582.